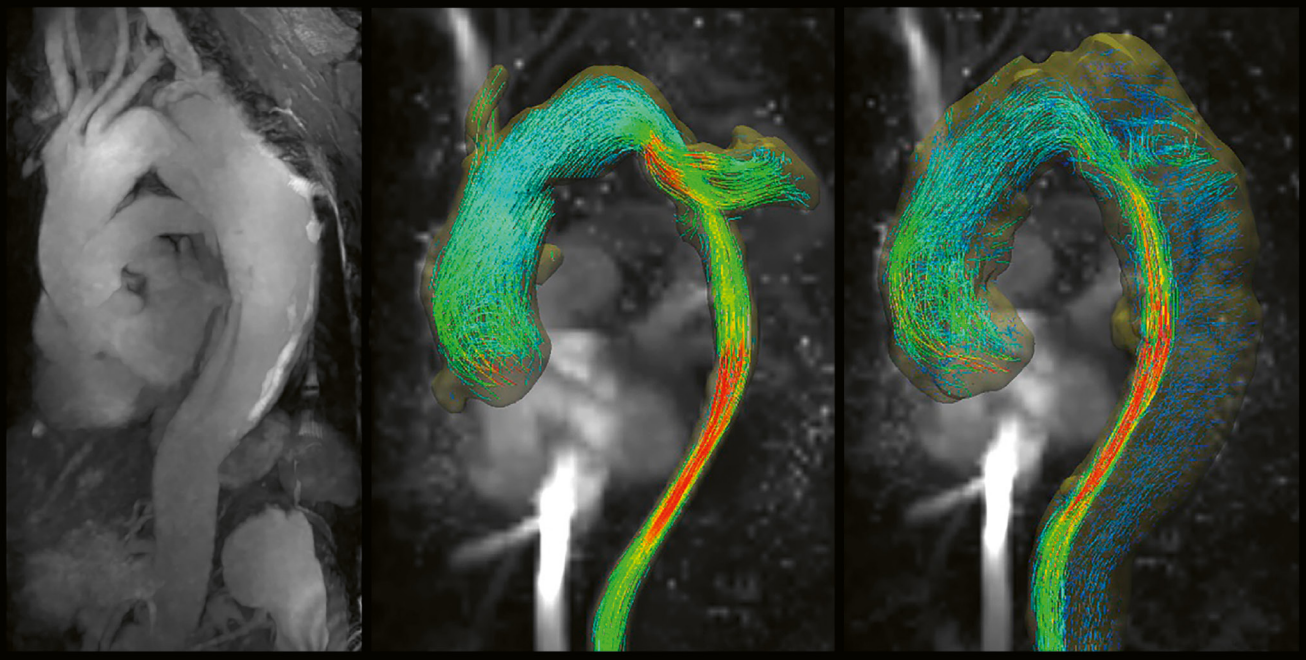

SMRA 2023

Clinical Benefits of MR Angiography

Clinical Impact of Combining Novel Non-Contrast-Enhanced MR Angiography with Multivenc 4D Flow MRI for Cardiovascular Diseases

Satoshi Higuchi, et al.
Tohoku University Hospital, Miyagi, Japan

Ferumoxytol-Enhanced 4D MRI in Pediatric and Adult Congenital Heart Disease

J. Paul Finn, et al.
David Geffen School of Medicine at UCLA, Los Angeles, CA, USA

Clinical Value of Free-Breathing Cardiac Cine MRI with Compressed Sensing Real-Time Imaging and Retrospective Motion Correction

Masahiro Takakado, et al.
Ehime Prefectural Central Hospital, Ehime, Japan

Artificial Intelligence: Learning About the Future of Cardiovascular MR

Kerstin Hammernik, et al.
Technical University of Munich, Germany / Imperial College London, UK

SIEMENS Healthineers

Prepare your patients mentally for their MRI exam

Most patients who undergo an MRI exam, experience some level of anxiety. As a result, some move so much that they cause motion artifacts, cannot complete the scan, or do not even show up for the exam. Up to 75%[1] of all unsatisfactory scan outcomes can be eliminated by educating patients on the MRI exam.

Tap the full potential of your facility by preparing your patients for the scan with our patient education toolkit. A **video, poster, meditation,** and a **book for children** explain the process of an MRI exam in simple words and answer common questions:

- What does an MRI exam entail?
- What is important when having an MRI exam?
- What does an MRI exam feel like?

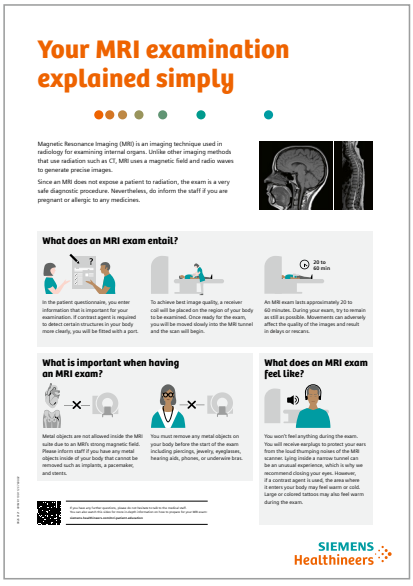

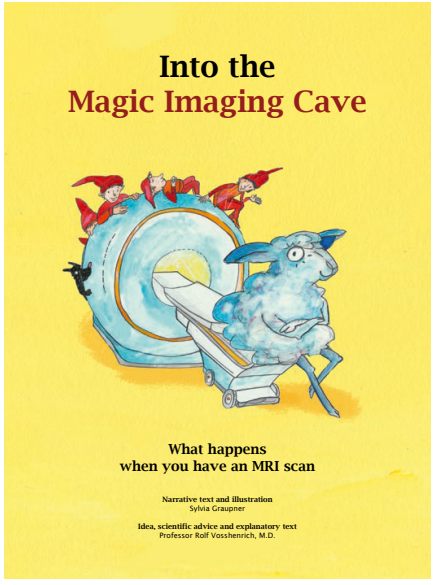

Download the patient education toolkit in your preferred language here:
siemens-healthineers.com/mri-patient-education

[1]*Törnqvist, E., Månsson, A., Larsson, E.-M., & Hallström, I. (2006). Impact of extended written information on patient anxiety and image motion artifacts during magnetic resonance imaging. Acta Radiologica, 47(5), 474–480. https://doi.org/10.1080/02841850600690355.*

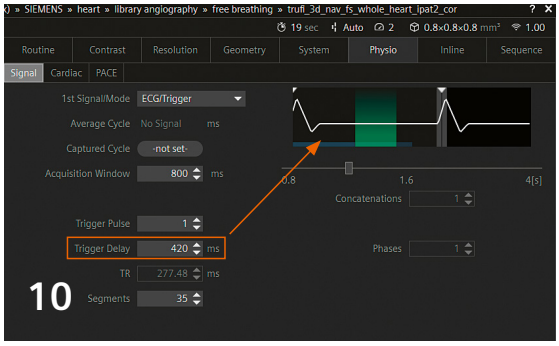

Trigger Delay, to achieve motion artifact free images in the heart region

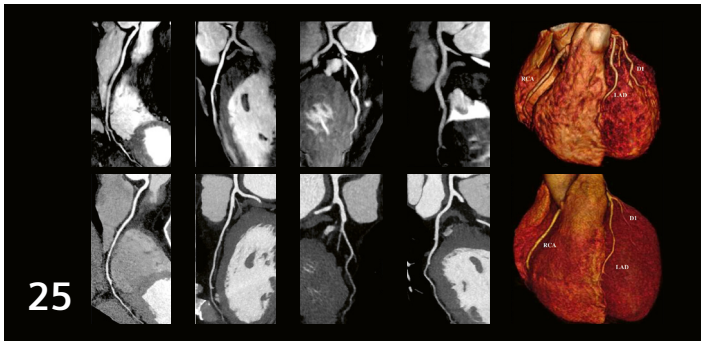

Curved multiplanar reformat and 3D volume-rendered non-contrast CMRA and contrast-enhanced CCTA

Cardiovascular Imaging

Expert Insights

Cardiovascular Imaging

Meet Siemens Healthineers

Clinical Impact of Combining Novel Non-Contrast-Enhanced MR Angiography with Multivenc 4D Flow MRI for Cardiovascular Diseases

Satoshi Higuchi[1], Yoshiaki Komori[2], Michaela Schmidt[3], Daniel Giese[3], Hideki Ota[1]

[1]Department of Diagnostic Radiology, Tohoku University Hospital, Miyagi, Japan
[2]Siemens Healthcare K.K., Tokyo, Japan
[3]Siemens Healthcare GmbH, Erlangen, Germany

Introduction

Non-contrast-enhanced magnetic resonance angiography (non-CE MRA) is a non-invasive examination which allows to visualize the vascular morphology and its vascularity without the ionizing radiation or administration of contrast agents required in CT angiography. Four-dimensional flow MRI (4D Flow MRI), which allows hemodynamic assessment in blood vessels, provides additional information for predicting cardiovascular events and understanding their pathology in patients with cardiovascular diseases.

However, these imaging techniques have the drawback of long scan times, due to the need for an electrocardiogram (ECG) and respiratory gating. Therefore, novel Compressed Sensing (CS) techniques and their application to non-CE MRA and 4D Flow MRI are emerging [1]. This paper reviews the clinical usefulness of highly accelerated non-CE MRA and highly accelerated 4D Flow MRI acquisition with multivenc (MV). These techniques will be termed *Advanced MRA* and *MV CS 4D Flow* in the following.

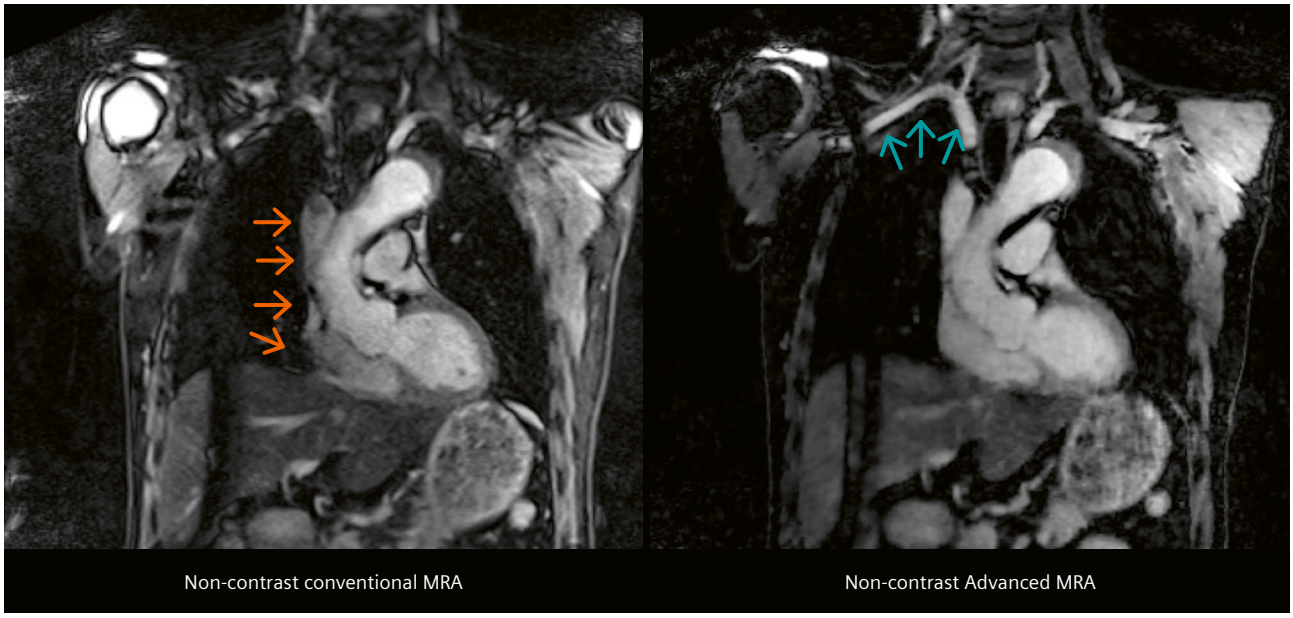

1 Comparison between conventional non-contrast MR angiography (MRA) and non-contrast Advanced MRA in a healthy volunteer.

Advanced MRA

Non-contrast MRA can be applicable to many patients with cardiovascular disease, but it is especially useful for imaging patients with congenital heart disease, patients with contraindications for contrast agent injection, and patients who need repeated follow-up imaging. However, the clinical use of free-breathing and ECG-gated native MRA acquisitions is often hampered by the long scan times needed to achieve high-resolution image quality. Siemens Healthineers recently introduced a novel non-CE MRA research sequence that uses Compressed Sensing (CS) and accurately reconstructs high-quality images from sparsely sampled *k*-space data with a significant reduction in scan time. The shorter scan time is expected to reduce motion artifacts, resulting in better image quality.

Furthermore, conventional MRA methods often use a spectral adiabatic inversion recovery (SPAIR) technique for fat suppression. This can cause non-uniform signal reduction in blood vessels due to the sensitivity to main magnetic field (B_0) inhomogeneities, especially at the boundaries of the lung and at locations with complex body morphology, such as the shoulders and neck [2]. Advanced MRA therefore uses a 2-point Dixon technique, which offers a robust fat-water separation technique that is less sensitive to B_0 inhomogeneity and therefore results in less signal inhomogeneity in the blood vessels and potentially improved diagnostic performance. Results from a volunteer show that the heterogeneous signal distribution in the right subclavian artery, superior vena cava, and ascending aorta in conventional MRA is improved using Advanced MRA (Fig. 1). Figure 2 shows the MRA results from a patient with partial anomalous pulmonary venous return (PAPVR) of the left upper pulmonary vein. The scan time for Advanced MRA was reduced to 7 minutes, compared to 26 minutes for conventional MRA. In Advanced MRA, the PAPVR is clearly visualized without the signal inhomogeneities seen around the apex of the left lung in the conventional MRA image. Thus, Advanced MRA is a promising and emerging imaging technique that is expected to be clinically useful for patients with cardiovascular disease. It clearly depicts vascular morphological and vascular course abnormalities in arteries and veins while reducing both scan time and any artifacts caused by motion and B_0 inhomogeneities.

MV CS 4D Flow

4D Flow MRI is an imaging technique that enables the visualization and quantification of physiological hemodynamics within the vasculature. While the assessment of vascular morphology using CTA has traditionally played a central role in diagnosis and treatment planning for vascular diseases, recent research efforts have focused on studying hemodynamics for further risk stratification and optimizing treatment strategies. Stanford type B aortic dissection is one of the diseases for which there is growing interest in developing hemodynamic biomarkers to predict prognosis. This is because evidence increasingly suggests that conservative management results in a favorable outcome in the acute phase, but a poor prognosis in the chronic phase [3–6]. We also retrospectively analyzed conventional 4D Flow MRI in patients with chronic Stanford type B aortic dissection and investigated the relationship between hemodynamic parameters at entry, true lumen, and false lumen and aortic growth rate derived from a CTA series (Fig. 3). This study revealed that patients with a

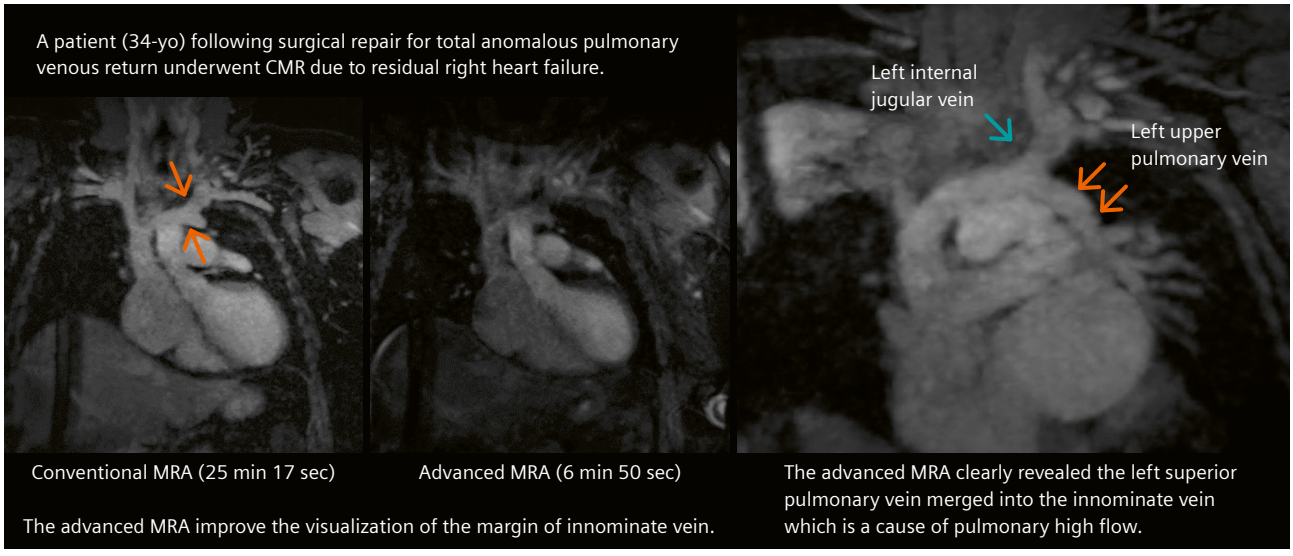

2 Partial anomalous pulmonary venous return (PAPVR), in which the left upper pulmonary vein drains into the left innominate vein.

higher rate of flow velocity or volume in the entry and false lumen compared to the true lumen were associated with fast aortic growth rate (Fig. 4) [7]. These hemodynamic parameters could be a new predictor of cardiovascular diseases. However, widespread clinical implementation of 4D Flow MRI is hindered by the long acquisition time and limited sensitivity to a large spectrum of velocities. These shortcomings can be addressed by applying CS in combination with a multivenc acquisition, which was recently included in the MV CS 4D Flow research sequence developed by Siemens Healthineers. Regularization is performed both in space and time. The shorter acquisition time makes it possible to perform the previously challenging multivenc scans, which acquire phase-contrast datasets with different velocity encoding (VENC) values within a single acquisition [8]. Figure 5 shows phase-contrast images for three different VENC values. Fast flow in the true lumen and entry, which cannot be depicted by the lower VENC due to aliasing, is clearly depicted by the higher VENC. Meanwhile, slow flow in the false lumen, which is not well depicted by the higher VENC due to a limited velocity-to-noise ratio (VNR), is clearly depicted by the lower VENC. The merged images are calculated using a Bayesian unfolding approach utilizing all phase-contrast images as well as their corresponding magnitude images to extract an optimal phase-contrast image. This image corresponds to the VNR-optimal combination of all single-VENC acquisitions and thereby accurately depicts a wide range of blood-flow velocities in a single series of images, complementing the limitation of each VENC setting (Figs. 6, 7).

Besides the long acquisition time, another reason for the limited clinical use of 4D Flow MRI is the post-processing with vessel segmentation. In conventional 4D Flow MRI, areas of slow blood flow are not recognized as intravascular regions, making it difficult to obtain accurate vessel segmentation easily (Fig. 8). By using the flow-independent vessel contrast of Advanced MRA and

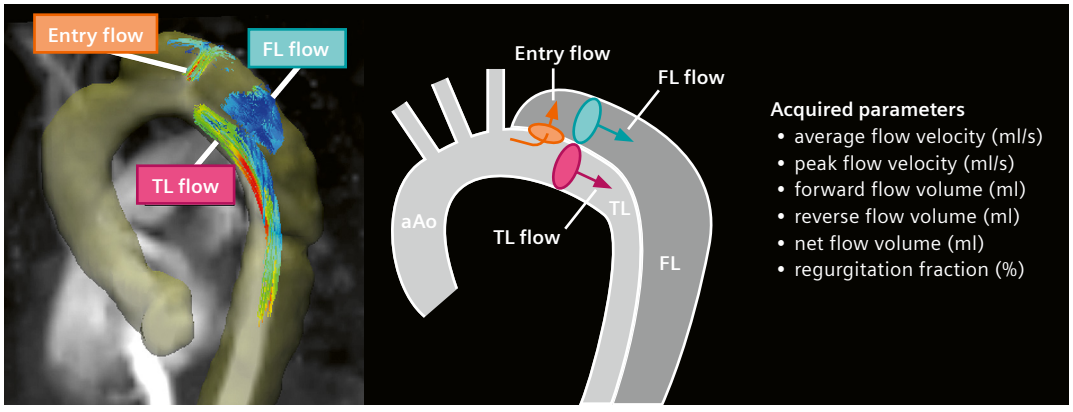

3 Evaluation of flow parameters in 4D Flow MRI in our study of patients with uncomplicated Stanford type B aortic dissection. TL: True lumen FL: False lumen

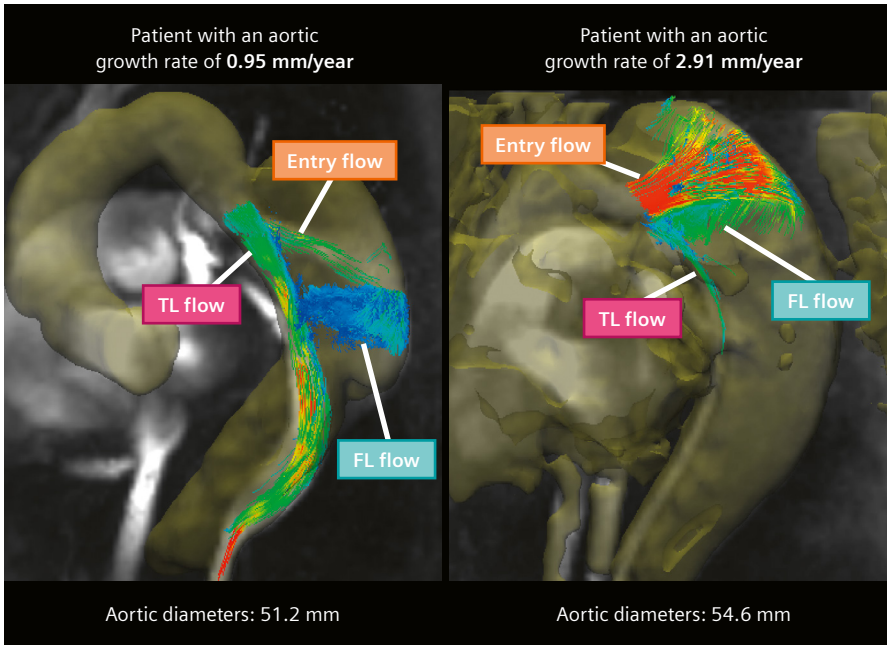

4 Patient with a low aortic growth rate demonstrates higher flow velocity and volume in true lumen (TL) than that in entry and false lumen (FL) (peak flow = 111, 23, and 83 mL/sec and net forward volume = 32, 5, and 16 mL in TL, entry, and FL, respectively). A patient with higher aortic growth rate shows lower flow in TL (peak flow = 45, 168, and 219 mL/sec and net forward volume = 16, 34, and 59 mL in TL, entry, and FL, respectively).

its higher resolution for segmentation, the 4D Flow analysis time can be reduced and vessels with low flow are optimally included in the segmentation for particle tracing.

Conclusion

The introduction of Advanced MRA and MV CS 4D Flow MRI is a groundbreaking advancement in cardiovascular imaging. In addition, as 4D Flow MRI becomes more widely available, more facilities will be able to perform it in clinical practice, and the accumulation of data from multiple facilities will accelerate the development of hemodynamic assessment methods. These non-invasive imaging techniques provide accurate diagnoses and hemodynamic information in vascular diseases in a shorter time and thus have the potential to transform trends in clinical

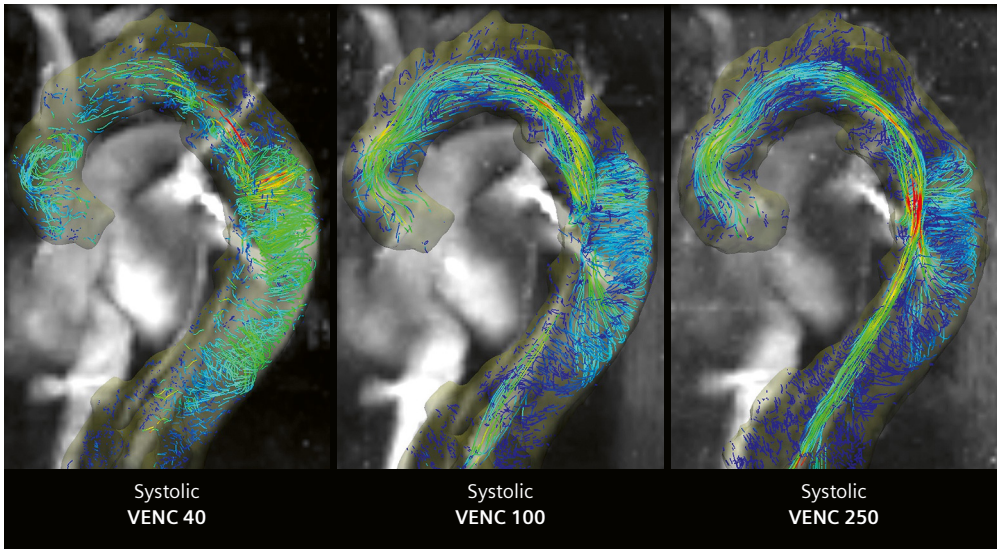

5 Differences in flow visualization in true lumen (fast flow) and false lumen (slow flow) due to differences in VENC settings.

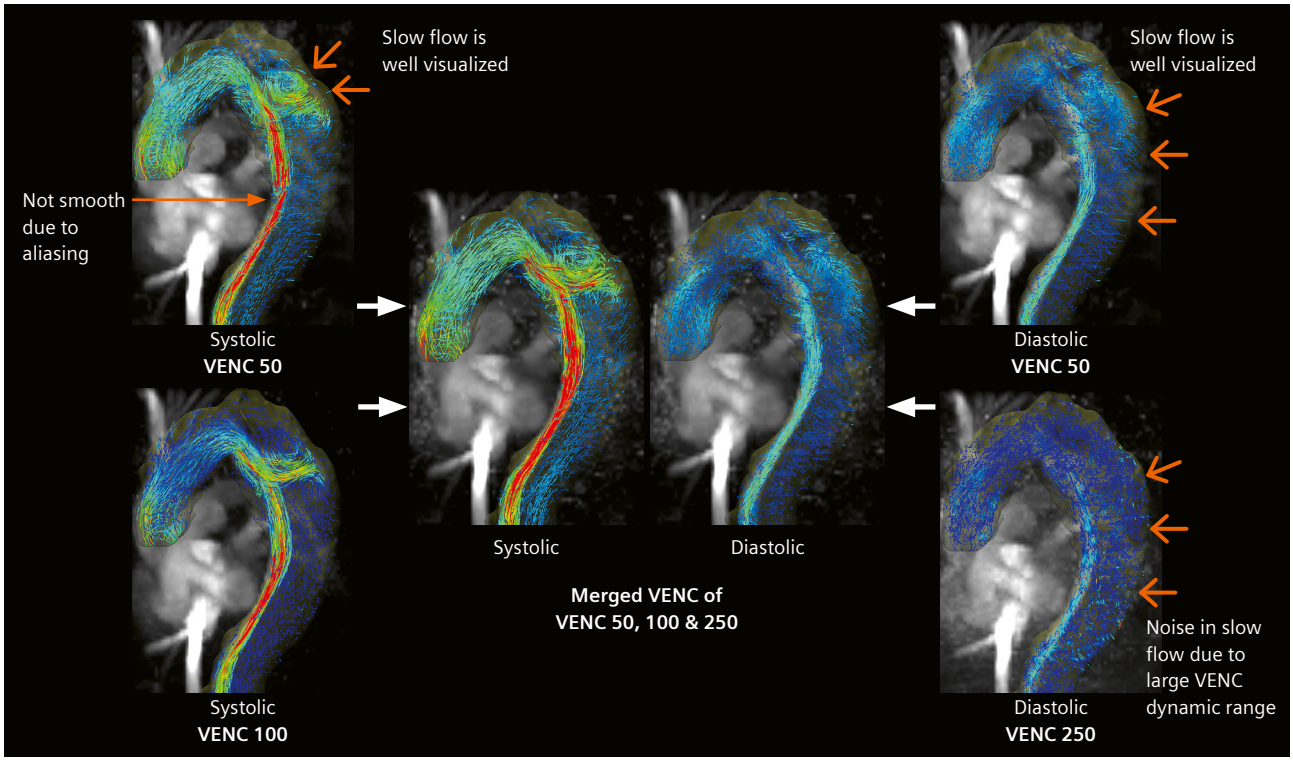

6 Merged VENC images are generated by synthesizing only the best signal from each dynamic range of the VENC images.

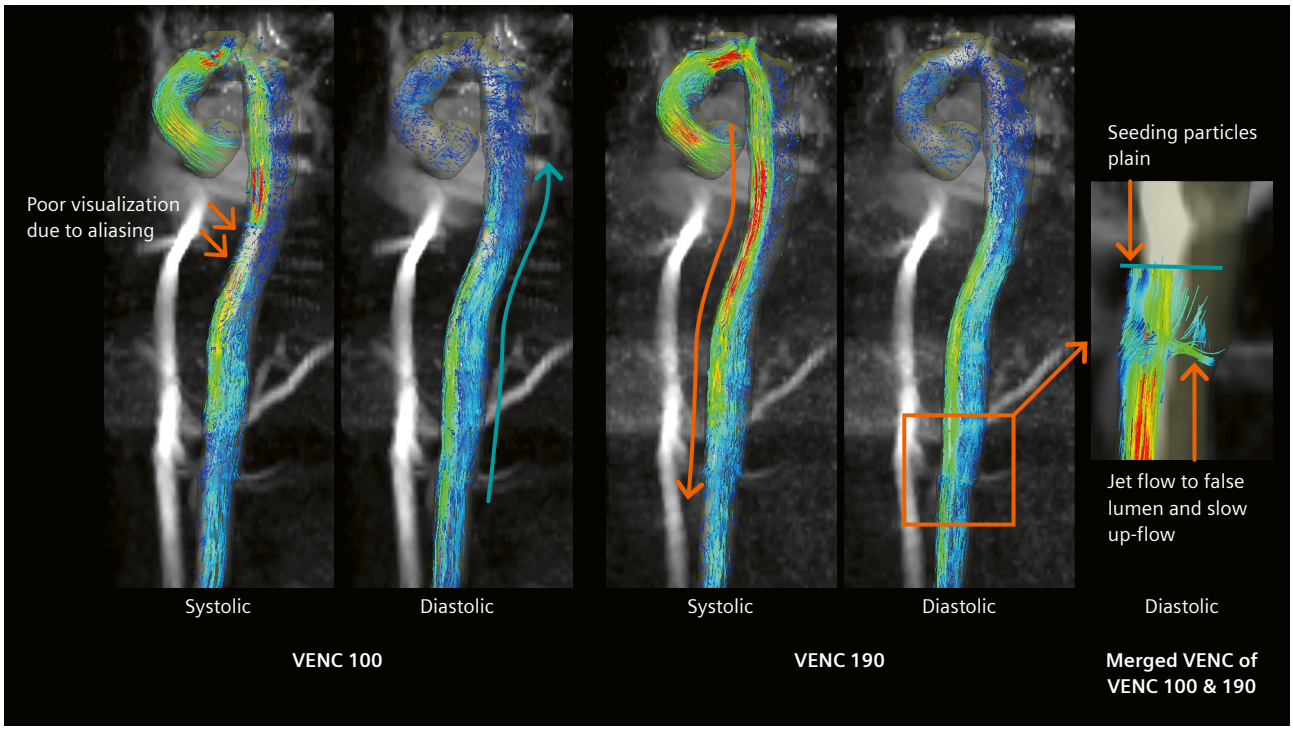

7 A merged VENC image visualizes the complex flow in both the true and false lumens.

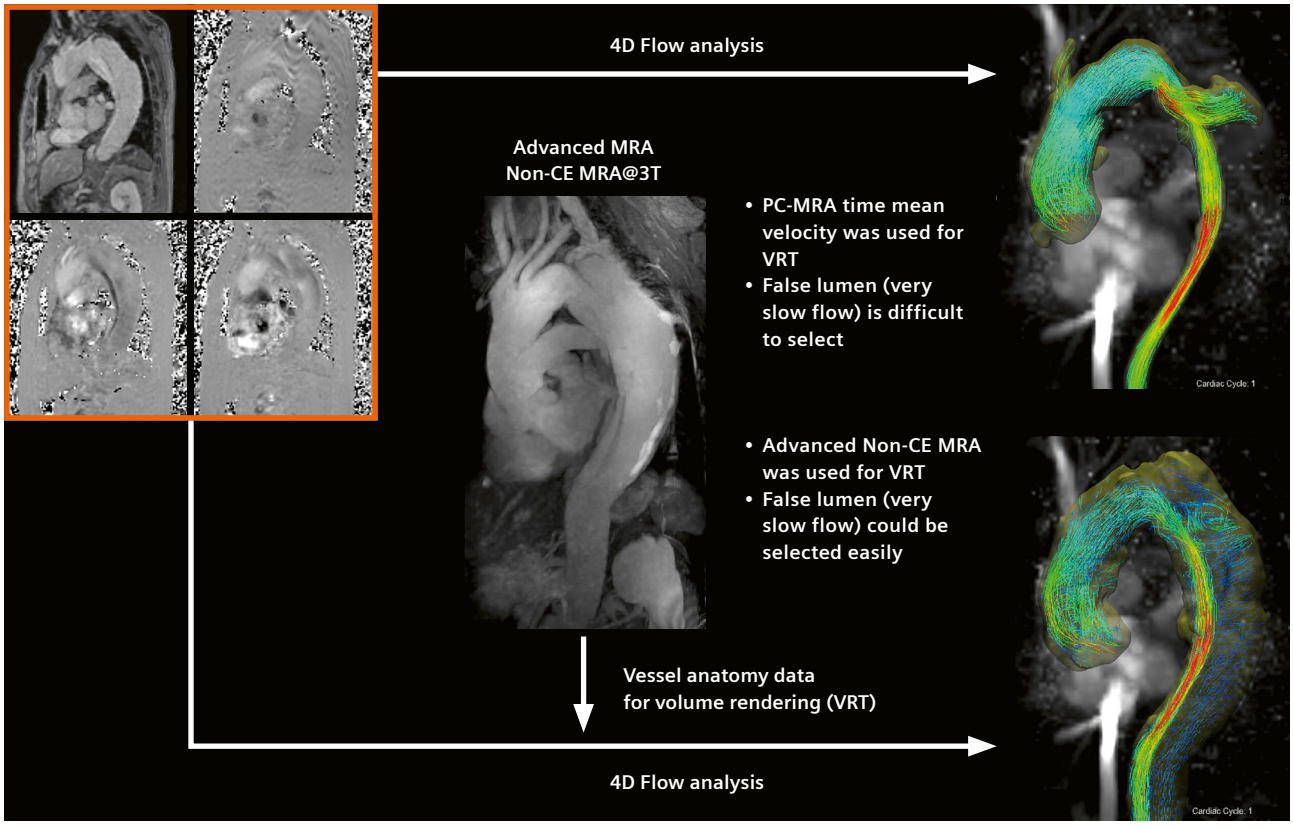

8 Improvement of 4D Flow postprocessing analysis using anatomical data with non-CE Advanced MRA.

	Advanced MRA	CS 4D Flow
Sequence type	T2-preped 3D FLASH	3D phase contrast cine
Acceleration technique	CS	CS
TE/TR (ms)	TE1 1.34, TE2 2.87/7.8	3.42/57.5
FOV (mm)	450 × 450	400 × 320
Image matrix	192 × 125	160 × 128
Reconstructed spatial resolution (mm)	1.2 × 1.2	2.5 × 2.5
Slice thickness (mm)	1.2	2.5
Slices per Slab	128	35
Orientation	Coronal	Sagittal
Flip angle (degrees)	12	7
Bandwidth (Hz/pixel)	799	558
Segments	25	1
Fat sat.	DIXON	–
Respiratory Gating	1D PACE, ± 6.5 mm	1D PACE, ± 8 mm, ReCAR
Acceleration factor	11	7.7
Iterative reconstruction (n)	20	30
VENC	–	dual or triple

Table 1: Imaging Parameters of Advanced MRA and CS 4D Flow
CS: compressed sensing, TE: echo time, TR: repetition time, FOV: field of view, VENC: velocity encoding, ReCAR: Respiratory Controlled Adaptive *k*-space Reordering.

practice by helping alleviate the patient burden and enhance overall workflow efficiency. Thus, these technologies hold great promise for improving patient management and advancing the field of cardiovascular medicine.

References

1 Feng L, Benkert T, Block KT, Sodickson DK, Otazo R, Chandarana H. Compressed sensing for body MRI. J Magn Reson Imaging. 2017;45(4):966-987.
2 Bley TA, Wieben O, François CJ, Brittain JH, Reeder SB. Fat and water magnetic resonance imaging. J Magn Reson Imaging. 2010;31(1):4-18.
3 Fleischmann D, Afifi RO, Casanegra AI, Elefteriades JA, Gleason TG, Hanneman K, et al. Imaging and Surveillance of Chronic Aortic Dissection: A Scientific Statement From the American Heart Association. Circ Cardiovasc Imaging. 2022;15(3):e000075.
4 Burris NS, Nordsletten DA, Sotelo JA, Grogan-Kaylor R, Houben IB, Figueroa CA, et al. False lumen ejection fraction predicts growth in type B aortic dissection: preliminary results. Eur J Cardiothorac Surg. 2020;57(5):896-903.
5 Evangelista A, Pineda V, Guala A, Bijnens B, Cuellar H, Rudenick P, et al. False Lumen Flow Assessment by Magnetic Resonance Imaging and Long-Term Outcomes in Uncomplicated Aortic Dissection. J Am Coll Cardiol. 2022;79(24):2415-2427.
6 Ruiz-Muñoz A, Guala A, Dux-Santoy L, Teixidó-Turà G, Servato ML, Valente F, et al. False lumen rotational flow and aortic stiffness are associated with aortic growth rate in patients with chronic aortic dissection of the descending aorta: a 4D flow cardiovascular magnetic resonance study. J Cardiovasc Magn Reson. 2022;24(1):20.
7 Satoshi H, Hideki O, Ryuichi M, Yuki I, Hiroki K, Kei T. Evaluation of hemodynamic parameters for prediction of aortic growth in patients with chronic Stanford type B aortic dissection using 4D flow MRI. In: Proceedings of the 31st Annual Meeting of ISMRM, Toronto, 2023. (abstract 1088).
8 Callaghan FM, Kozor R, Sherrah AG, Vallely M, Celermajer D, Figtree GA, et al. Use of multi-velocity encoding 4D flow MRI to improve quantification of flow patterns in the aorta. J Magn Reson Imaging. 2016;43(2):352-363.

Contact

Satoshi Higuchi, M.D., Ph.D.
Tohoku University Hospital
Department of Diagnostic Radiology
1-1 Seiryomachi, Aoba, Sendai, Miyagi
Japan
Tel: +81-22-717-7312
satoshi.higuchi.b4@tohoku.ac.jp

Expert Insights: Hidden Gems from Application Specialists at Siemens Healthineers

Khaled Khames on the Trigger Delay parameter

Khaled Khames

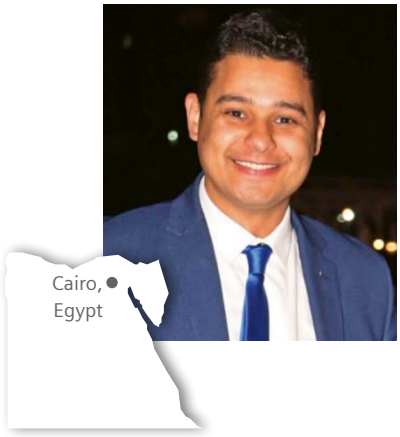

Khaled Khames is a physicist in Cairo, Egypt. He is passionate about training clinical staff on new MR technologies to help build MR expertise and practices that achieve the best outcomes for patients and optimal performance for healthcare providers.

Khaled enrolled in a Bachelor of Science in 2006, at the Department of Physics at Ain Shams University in Cairo. He went on to work as a physicist in a diagnostic nuclear medicine unit. When he discovered MRI, however, he was fascinated by the evolving technology and the challenges it solved, all of which inspired him to embark on a career in the MR field.

This path eventually led him to Siemens Healthineers, where he became Senior Application Specialist for Egypt, Sudan, Libya, Eritrea, and Djibouti in 2015. He is also an instructor at the Siemens Healthineers Academy in Egypt, where he teaches basic and advanced MR courses for physicians and technologists.

Khaled received the Learn Passionately Award 2023 at the Egypt Mid-Year townhall meeting. Outside of work, he loves spending time with his three daughters and going fishing.

Contact

Khaled Khames
Siemens Healthcare S.A.E.
SHS EMEA MESA EGY CS 1
Etisalat Club Rd
11435 al-Qahirah
Postbox 17631 Maadi
Cairo
Egypt
khaled.khames@siemens-healthineers.com

My favorite feature ...

... is the Trigger Delay parameter, to achieve motion artifact free images in the heart region. You can use it to optimize image quality in noncontrast-enhanced MR angiography when using a triggered 3D TrueFISP or FLASH sequence – to image the whole heart, coronaries, or the aorta.

The Trigger Delay should be set in such a way, that the region of interest is in a quiet phase, i.e., not much heart motion or flow happening during data acquisition.

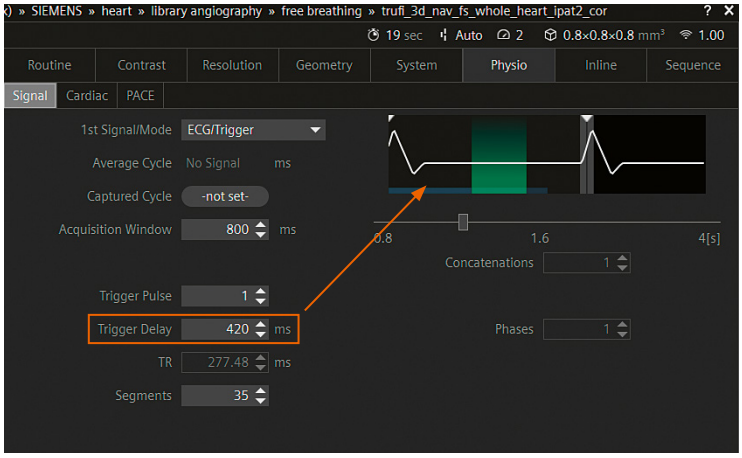

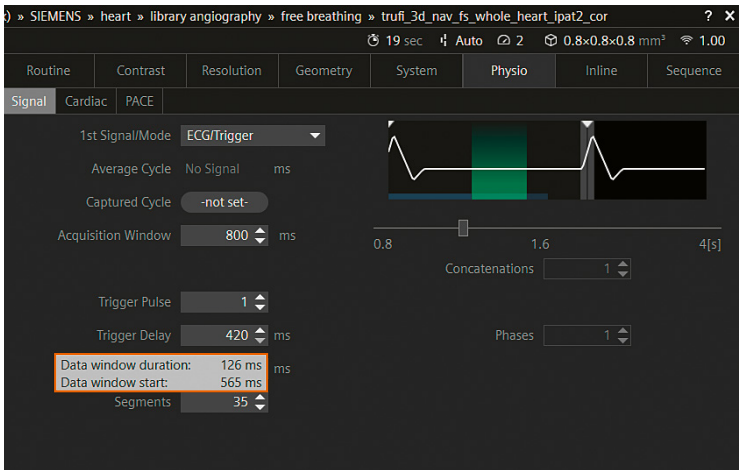

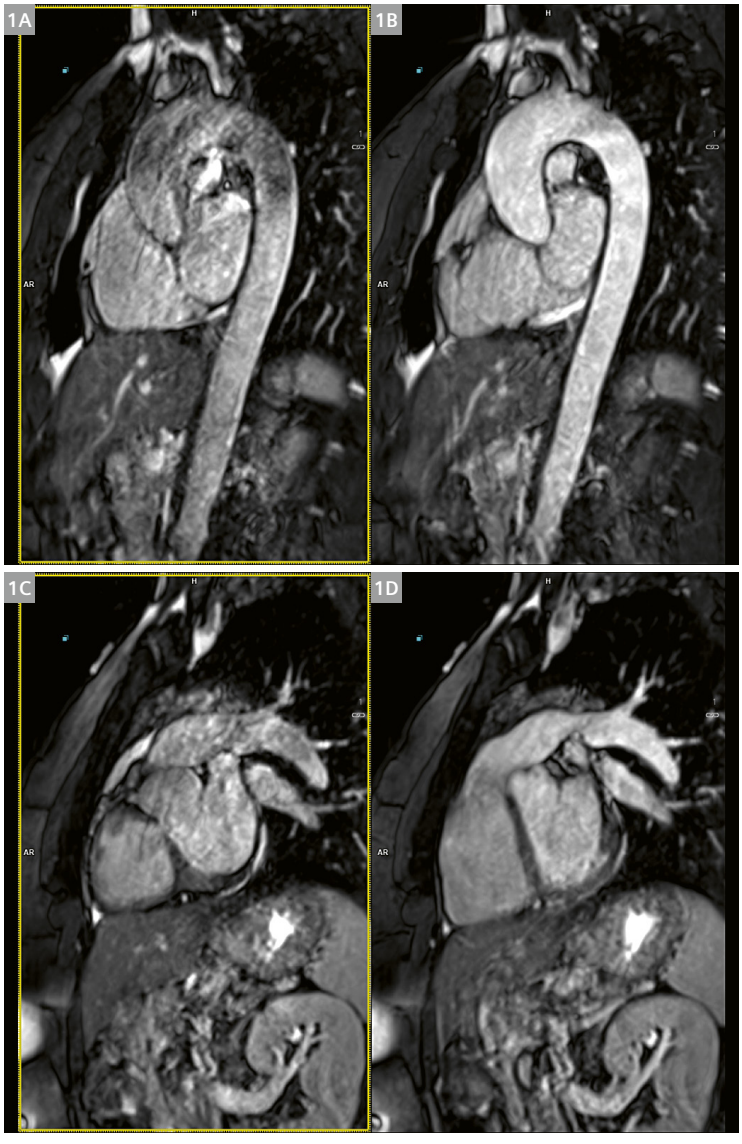

1 Noncontrast triggered 3D TrueFISP
(1A) Suboptimal Trigger Delay time, **(1B)** Appropriate Trigger Delay time, **(1C)** Suboptimal Trigger Delay time, **(1D)** Appropriate Trigger Delay time

This quiet phase can be identified by a visual assessment of cine or flow images from the corresponding region. Scroll through the cine images and identify the quiet phase, ideally with starting and end point and the length in ms. The TT (Trigger Time) can be found in the image text on the left side.

With this knowledge you can now individually optimize the parametrization of the 3D sequence to the patients' condition on the parameter card Physio/Signal.

Before you start editing, hover with the mouse cursor over the Trigger Delay parameter to visualize the information of the Data window start and the Data window duration.

Adapting the Trigger Delay shifts your Data window start. (Cave: Additional Prep Pulses are added to the Trigger Delay for the Data window start point, such that the shown Trigger Delay in the user interface (UI) is not corresponding to the Data window start).

Adapting the number of segments modifies the Data window length. Modifying the number of segments has an impact on the Data window duration and the total acquisition time.

Number of segments ↑
Data window duration ↑
Total acquisition Time ↓

Number of segments ↓
Data window duration ↓
Total acquisition Time ↑

It is recommended to use a Data Window duration between 100 and 180 ms to keep motion and flow artifacts minimal.

Cave: Use a consistent trigger source. If you use e.g., Beat Sensor for cine imaging, make sure to use Beat Sensor for 3D imaging, too.

Acknowledgments

I would like to acknowledge the fruitful conversations with Manuela Rick, Senior Applications Developer, Erlangen, Germany

Ferumoxytol-Enhanced 4-Dimensional MR Imaging in Pediatric and Adult Congenital Heart Disease

J. Paul Finn, M.D.[1,2]; Takegawa Yoshida, M.D.[1]; Arash Bedayat, M.D.[1]; Ashley Prosper, M.D.[1]; Chang Gao[1]; Xiaodong Zhong, Ph.D.[1]; Ning Jin, Ph.D.[3]; Xiaoming Bi, Ph.D.[4]; Kim-Lien Nguyen, M.D.[1,2,5]

[1]Diagnostic Cardiovascular Imaging Laboratory, Department of Radiological Sciences, David Geffen School of Medicine at UCLA, Los Angeles, CA, USA
[2]Physics and Biology in Medicine Graduate Program, University of California, Los Angeles, CA, USA
[3]MR R&D Collaborations, Siemens Medical Solutions USA, Inc., Cleveland, OH, USA
[4]MR R&D Collaborations, Siemens Medical Solutions USA, Inc., Los Angeles, CA, USA
[5]Division of Cardiology, David Geffen School of Medicine at UCLA and VA Greater Los Angeles Healthcare System, Los Angeles, CA, USA

Introduction

MRI has unique strengths for cardiac imaging and is particularly useful in patients with congenital heart diseases. In recent years, multidimensional cardiac imaging has shown spectacular results by combining advanced techniques with ferumoxytol[1] enhancement of the blood pool. In this short report, we will show how 4-dimensional imaging can be applied successfully to children[2] and adults with congenital heart disease (CHD), with one illustrative example in each respective category.

Children with congenital heart disease

In children, our goal is high-resolution, artifact-free images over the full cardiac cycle in patients who may weigh less than 2 kg, whose heart rate may exceed 180 beats per minute, who breathe up to 40 times per minute, and who may move spontaneously at any time. What could possibly go wrong!

The holy grail is to perform these studies without sedation while the patient breathes spontaneously. Intensive research is underway in many laboratories (including our own) to make this a reality [1–7], but significant technical challenges remain. Meanwhile, with certain constraints, detailed and comprehensive 4-dimensional MR imaging of children with CHD is possible today, using a well-established methodology. The approach we have adopted is simple and consistent for all children who require sedation, independent of patient size, age, or disease complexity. The key components include:

1. Enhancement of the blood pool in the steady state distribution of ferumoxytol
2. A controlled and regular respiratory pattern, ensured by positive pressure ventilation and muscle relaxants
3. Cardiac-triggered and respiratory-gated volumetric acquisitions over all desired anatomy with 4D MUSIC[3] [8] and 4D flow[4] (non-product) sequences, during uninterrupted ventilation

With the sequences we use, image reconstruction is inline and immediate, although the 4D flow images require advanced processing with commercial software. We use Arterys (Tempus, Chicago, IL, USA) for 4D flow processing, but other commercial options are available. The MUSIC images are immediately available as DICOM input to any platform with a 4D viewing option, where 2D cines can be reconstructed in any plane and saved to an archival (PACS) system. We use OsiriX (Pixmeo SARL, Bernex, Switzerland) on a Mac workstation.

[1] Ferumoxytol is not approved for diagnostic applications and its use for MRI is off-label.
[2] MR scanning has not been established as safe for imaging fetuses and infants less than two years of age. The responsible physician must evaluate the benefits of the MR examination compared to those of other imaging procedures. Note: This disclaimer does not represent the opinion of the author.
[3] MUSIC is a prototype sequence developed at UCLA.
[4] The authors are using a non-product sequence, but 4D Flow has been available as a product since software version syngo MR XA30.

In our practice, the typical imaging time from the first scout sequences to completion of the last series is less than 30 minutes, without any requirement for breath-holding and irrespective of how complex the disease is. The covered anatomy includes the heart and the blood vessels of the neck, chest, and abdomen. For context, conventional imaging with 2D cine, 3D contrast-enhanced MRA, and targeted 2D flow requires repeated breath-holding and interactive scanning prescription that may take 60 to 90 minutes. Moreover, in the end, it may be that certain image planes that in hindsight were relevant had not been acquired and cannot be retrospectively reconstructed. With the 4D approach, this is never the situation.

Case 1

A 22-month-old[1] male patient with heterotaxia and double outflow right ventricle (DORV) had undergone bilateral Glenn shunt procedures and was being assessed for possible bi-ventricular repair. MRI was requested to define cardiac chamber anatomy and size, vascular anatomy, and the integrity of the Glenn shunts. The patient underwent general anesthesia, intubation, and controlled ventilation, and received ferumoxytol, 4 mg/kg, by slow intravenous infusion before being advanced into the bore of a 3T MAGNETOM Trio scanner (Siemens Healthcare, Erlangen, Germany). A small flex coil was positioned over the heart, and continuous monitoring of ECG, pulse oximetry, airway pressure, and non-invasive blood pressure was performed. Following initial scout images, a real-time cine series in the coronal plane was acquired over 20 seconds to confirm satisfactory ventilatory movement of both hemi-diaphragms. A 4D MUSIC acquisition [8] was then performed encompassing the neck, chest, and abdomen. Non-interpolated spatial resolution was 1 mm isotropic, and 11 cardiac phases were acquired, gated to end-expiration. Following the MUSIC acquisition, a 4D flow sequence was run with 1.7 × 1.7 × 1.9 mm (non-interpolated) voxels and 45 ms temporal resolution, also during uninterrupted ventilation and gated to end-expiration. The respiratory gating efficiency for both 4D sequences was 60% and the total acquisition time was 20 minutes (8 minutes for MUSIC and 12 minutes for 4D flow). The MUSIC DICOM images were pushed to OsiriX, Vitrea (Rishon LeZion, Israel), and Mimics (Materialise, Leuven, Belgium) workstations for multi-planar cine recon (OsiriX), volume rendering (Vitrea), and quantitative segmentation of chamber sizes (Mimics). The 4D flow DICOM images were uploaded to the Arterys cloud for processing.

Results

The MUSIC images confirmed heterotaxia with a left-sided inferior vena cava (IVC), right-sided aortic arch, and distended hepatic veins draining to the right atrium (Fig. 1).

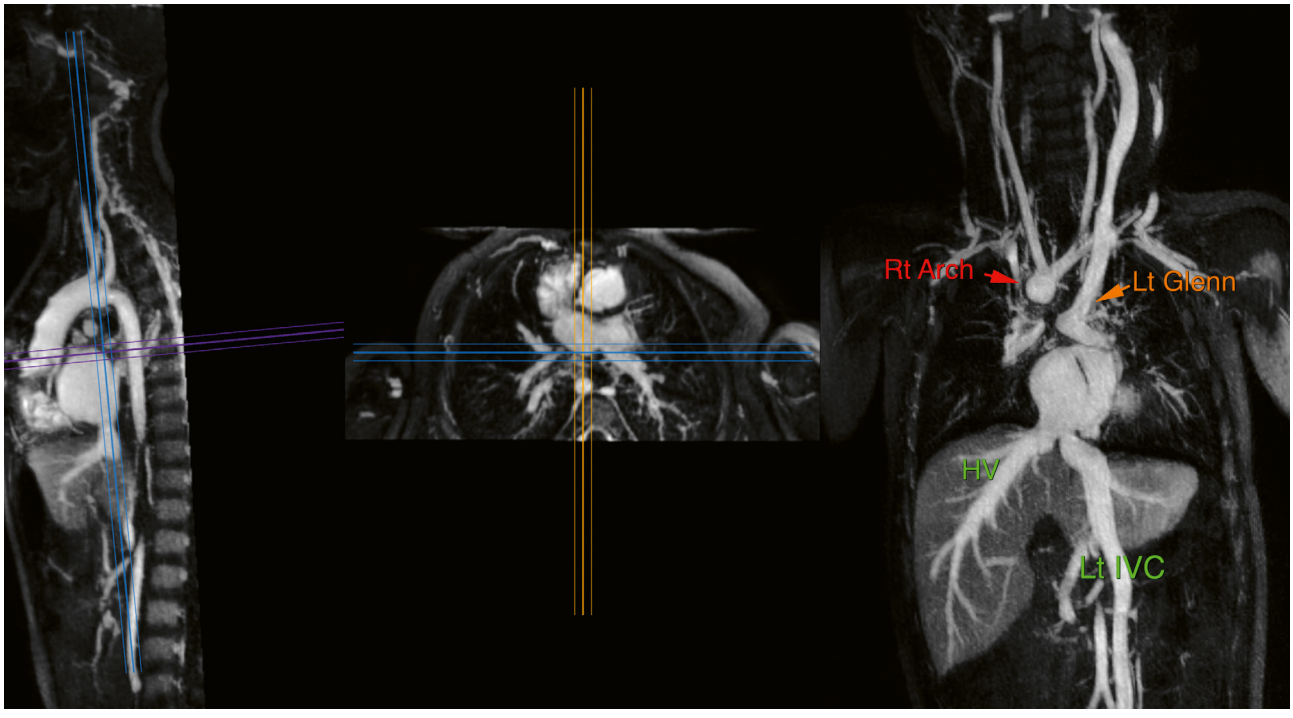

1 Thin MIP reconstructions from the 4D MUSIC acquisition in OsiriX showing the venous anatomy and the right-sided aortic arch (HV: hepatic vein; Lt IVC: left inferior vena cava; MIP: maximum intensity projection).

Dynamic cardiac chamber anatomy was clearly shown, and chamber volumes were confidently measured (Fig. 2). 4D flow confirmed normal hemodynamics in the aorta and branches, and documented the outflow pattern from the left ventricle to the aorta (Fig. 3). The origins and courses of the coronary arteries were conventional (Fig. 4). The left Glenn shunt was widely patent with appropriate flow (Fig. 5). The right Glenn was small, stenosed, and non-functional with minimal flow (Fig. 6). 3D frames from the MUSIC data were printed to help in surgical

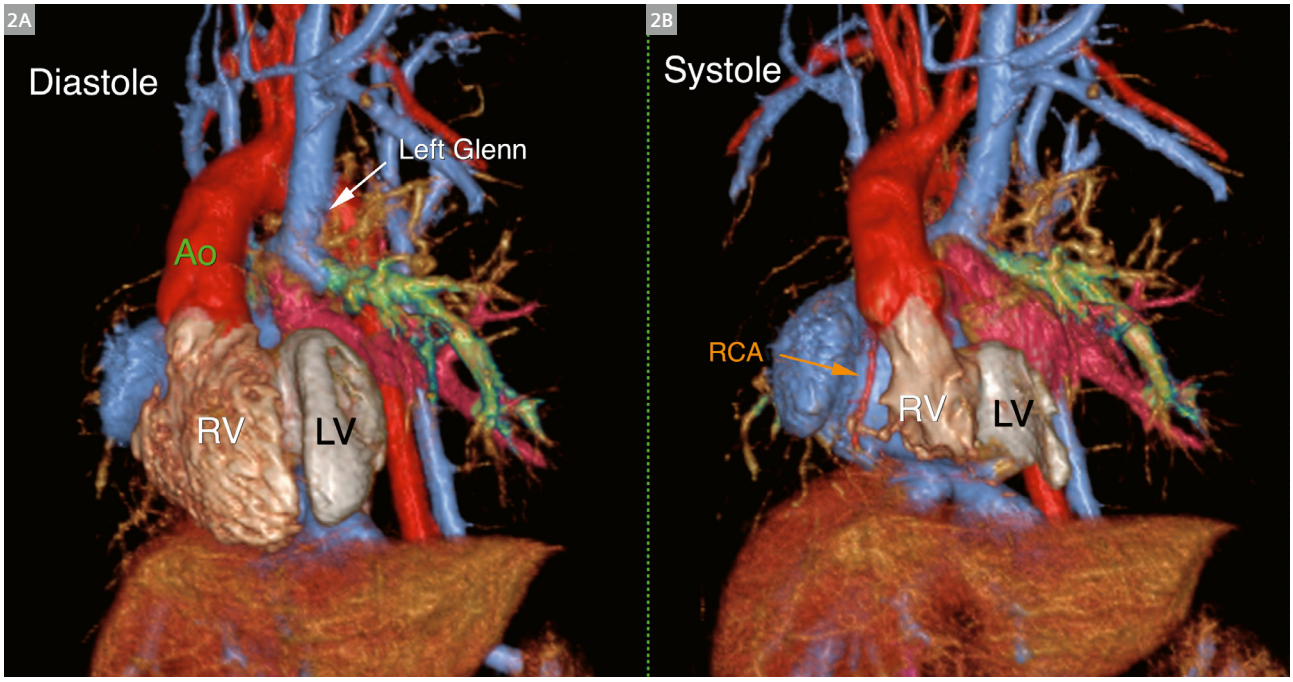

2 Color volume-rendered reconstructions (Vitrea) of the heart and great vessels in diastole **(2A)** and systole **(2B)** show the left Glenn shunt, aorta (Ao), left ventricle (LV), right ventricle (RV), and right coronary artery (RCA).

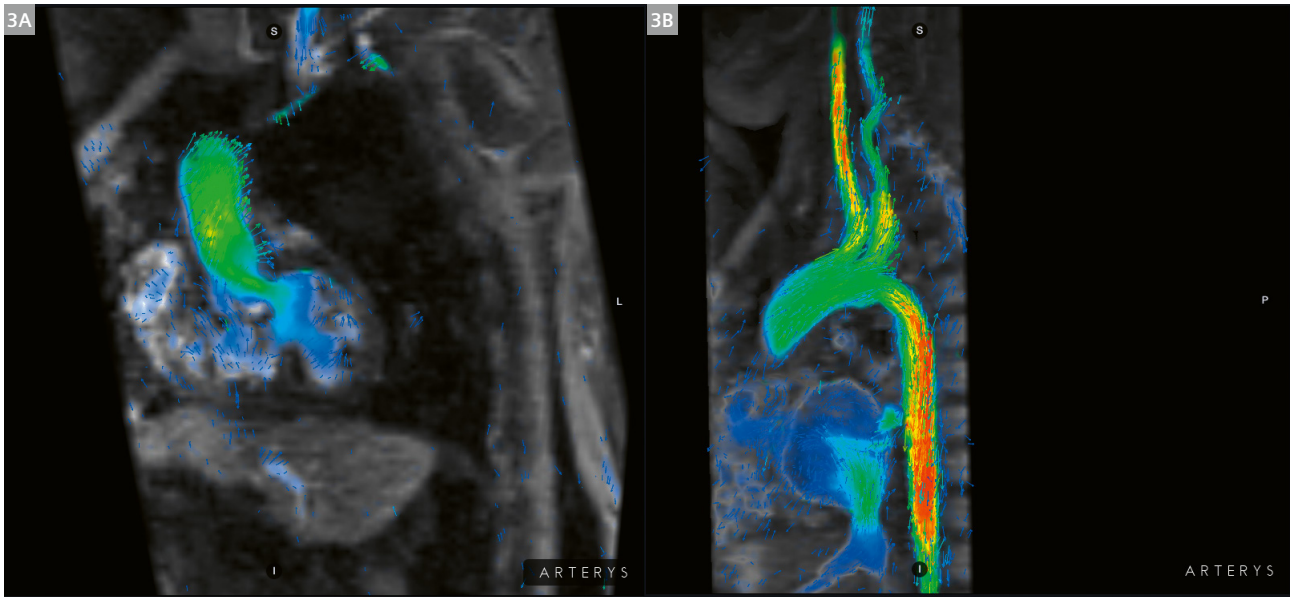

3 Frames reconstructed from the 4D flow data (Arterys) show the outflow pathway from the left ventricle to the Aorta (**3A**, oblique coronal) and normal flow patterns in the aortic arch and great vessels (**3B**, oblique sagittal).

planning and procedure simulation. Movie files for all figures are available as an online supplement at https://www.magnetomworld.siemens-healthineers.com/clinical-corner/case-studies/ferumoxytol.

It is important to note that, in addition to the specific findings noted above in this patient, the steady state of ferumoxytol makes every vessel in the chest, neck, abdomen, and pelvis clearly assessable.

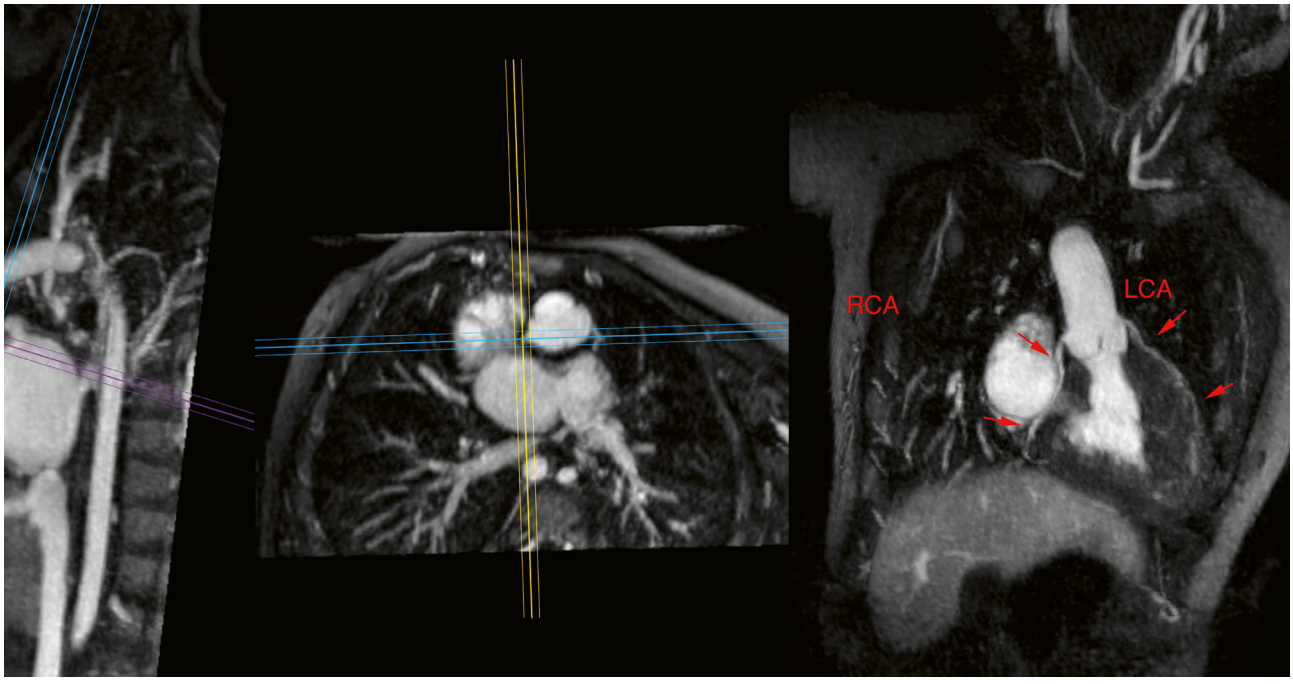

4 Thin MIP reconstructions from the 4D MUSIC acquisition in OsiriX showing the right coronary artery (RCA) and left coronary artery (LCA).

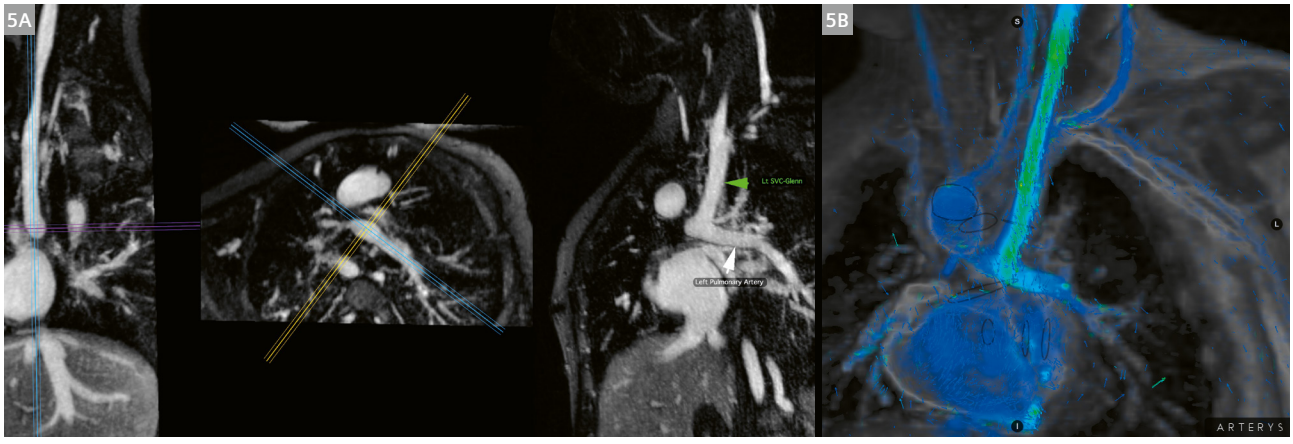

5 Thin MIP reconstructions from the 4D MUSIC acquisition in OsiriX show anatomy of the intact left Glenn shunt **(5A)**, and a frame from the 4D flow shows appropriate flow in the left Glenn (Arterys).

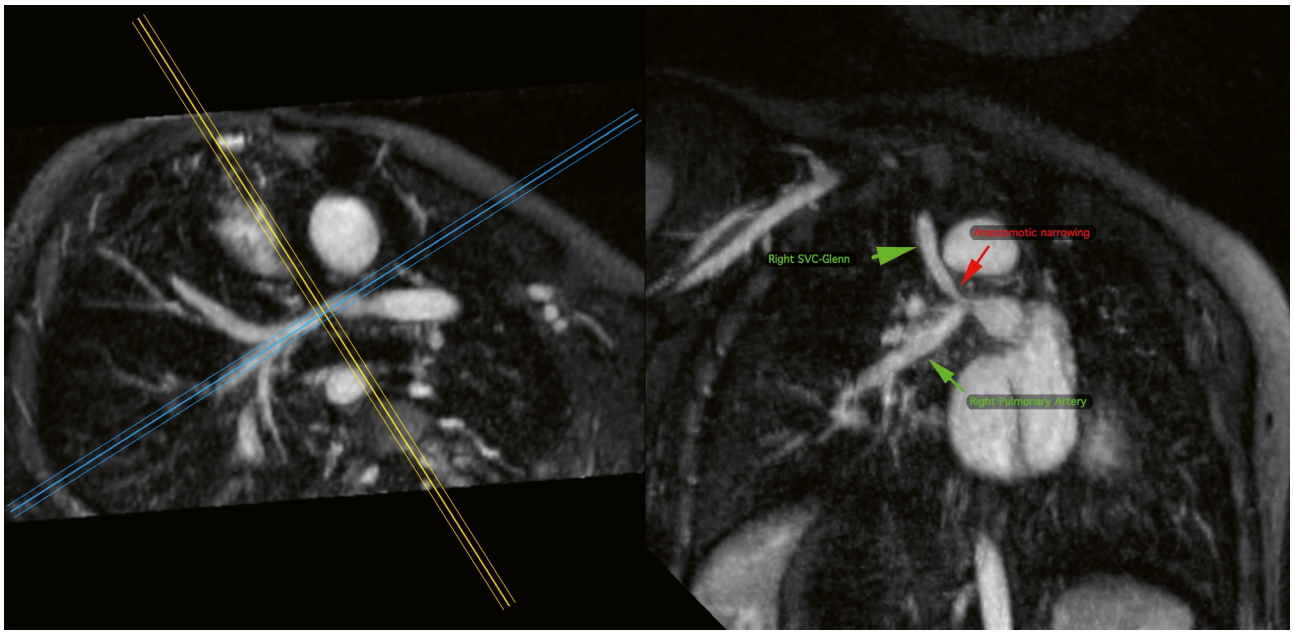

6 Thin MIP reconstructions from the 4D MUSIC acquisition in OsiriX show anatomy of the stenosed right Glenn shunt and the stenosed origin of the right pulmonary artery.

Adults with congenital heart disease

Whereas anesthesia and controlled ventilation solve the motion artifact problem in small children, we must use different tools in adults. Breath holding is generally very effective for 2D or 3D imaging, but for 4D flow imaging, some form of respiratory gating or compensation is needed. Recent advances in compressed sensing (CS) show great promise for highly accelerated 4D flow imaging and ferumoxytol enhancement can mitigate much of the SNR penalty that aggressive undersampling imposes. In the example below, we illustrate how CS 4D flow and ferumoxytol combine to generate high quality data in a practical acquisition time.

Case 2

A 30-year-old male patient with congenital bicuspid aortic valve had undergone valve-sparing surgery for an ascending aortic aneurysm. Follow-up echocardiography showed aortic valve incompetence, and the patient was referred to MR for a more detailed evaluation. The study was performed on a 1.5T MAGNETOM Sola (Siemens Healthcare, Erlangen, Germany). Following infusion of 4 mg/kg of ferumoxytol, the patient was advanced into the scanner bore, with two body array coils in place. The routine clinical acquisition protocol included multiplanar cine with breath-hold SGE (FLASH), 3D MRA, 2D flow imaging through the aortic valve, and non-breath-hold HASTE imaging. 4D flow imaging was then performed using a research sequence that incorporates compressed sensing (CS) acceleration and a diaphragmatic navigator for respiratory gating. A CS acceleration factor of 12.8 was used in the current study. Spatial resolution was 2 mm isotropic (non-interpolated) and temporal resolution was 48 ms. ECG retro-gating was employed, and 20 cardiac phases were calculated.

Results

Cine confirmed the bicuspid aortic valve (Fig. 7A) and MRA showed satisfactory appearances of the surgical aortic graft (Fig. 7B). Respiratory gating efficiency for the 4D flow acquisition was 65% and the total acquisition time was 5 minutes 40 seconds. The image quality for the 4D flow acquisition was excellent, with high SNR for all vascular structures (Fig. 8). The aortic regurgitation fraction for both the 2D and 4D flow measurements was in full agreement at 43%. The 4D flow additionally showed the 3D geometry of the regurgitation jet, and provided a graphic depiction of the volumetric flow fields in the aorta, pulmonary artery, and included cardiac chambers. MRA confirmed the integrity of the surgical aortic graft repair, and cine imaging confirmed the congenitally bicuspid nature of the aortic valve. Additionally, cine and HASTE showed left ventricular non-compaction, not appreciated on echo.

In children with CHD, ferumoxytol has ushered in a paradigm shift for MRI. Because of its long half-life in the blood, ferumoxytol supports high-resolution 4D imaging and has been used successfully in several centers at both 3T and 1.5T [9, 10]. When implemented with cardiac and respiratory gating, high-dimensional techniques such

as MUSIC and Free-Running Framework [5] can produce images with uniformly high contrast throughout the cardiac chambers and blood vessels.

Ferumoxytol enhancement lays the groundwork for uniformly high vascular signal without concerns for saturation of the blood. This effect gives a new lease of life to the entire family of T1-weighted spoiled gradient echo (SGE, FLASH) sequences that are tolerant of magnetic field non-uniformities and artifacts from devices. Moreover, the benefits apply to all field strengths. The high blood SNR also supports more aggressive under-sampling schemes for parallel imaging and, as shown in our adult case above, for compressive sensing in 4D flow. In the adult patient illustrated above, the 4D flow acquisition used an acceleration factor of 12.8, while maintaining high signal on the bright blood magnitude images. The same mechanism that supports high signal on the magnitude images supports more reliable estimation of flow-induced phase shifts, since the phase is less noisy if the magnitude signal is high [11]. It should be noted that ferumoxytol

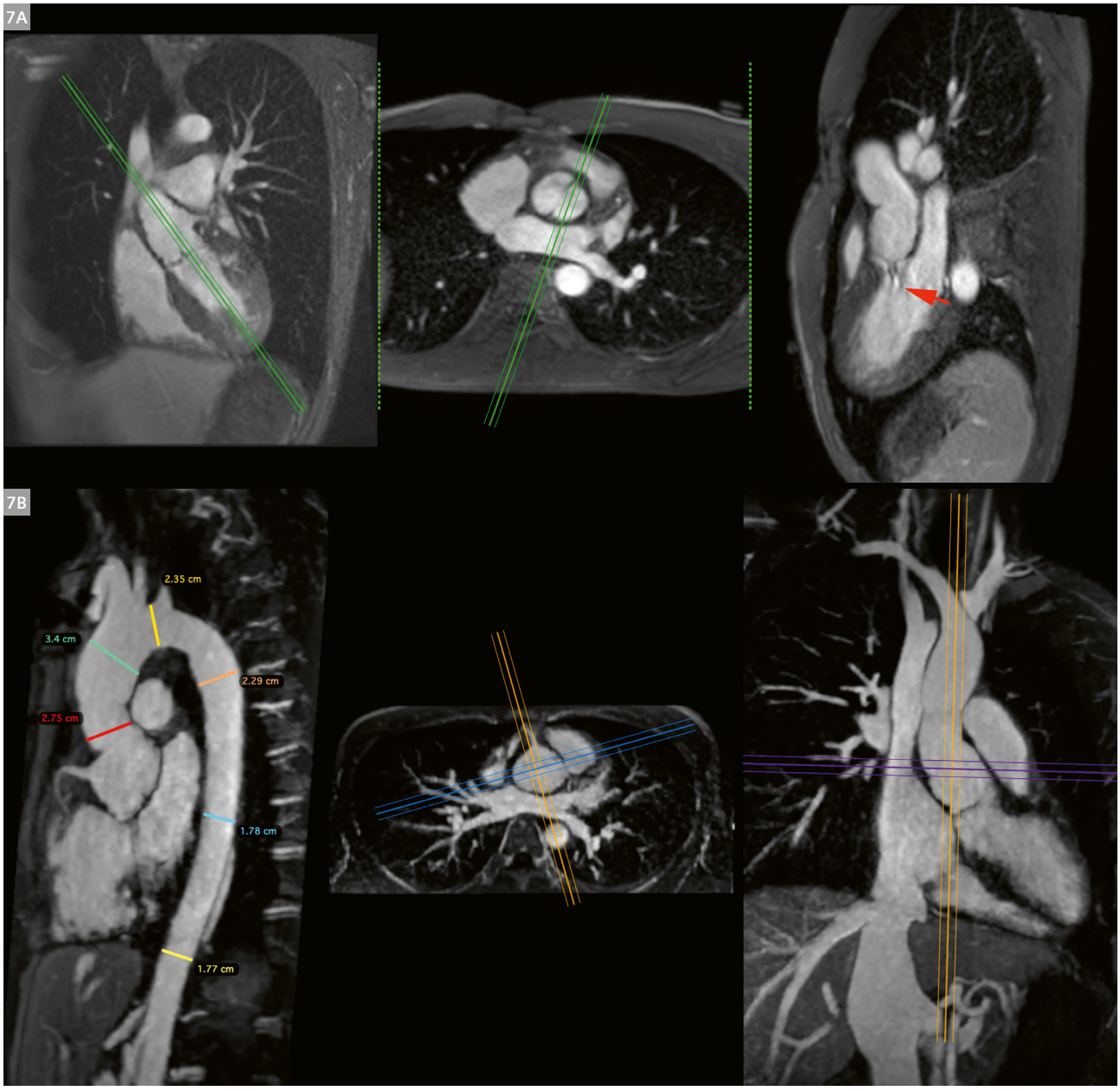

7 **(7A)** 30-year-old male patient with bicuspid aortic valve. Diastolic frames from 2D FLASH cine show the bicuspid aortic valve (middle panel) and aortic regurgitant jet (right panel). **(7B)** 30-year-old male patient with bicuspid aortic valve. Thin MIP reconstructions from gated MRA (OsiriX) post-ferumoxytol show the dimensions of the ascending aortic surgical graft and thoracic aorta (left panel).

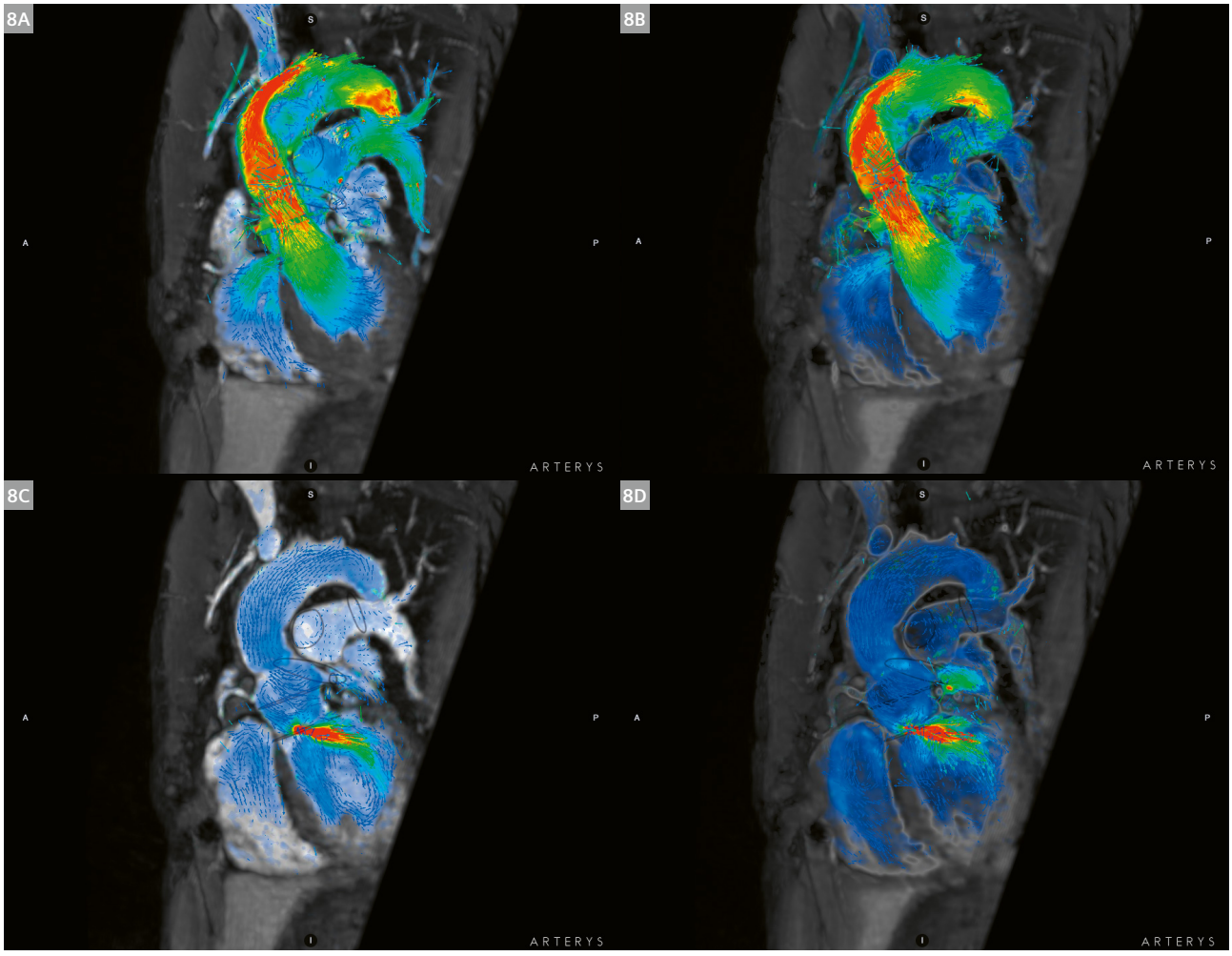

8 30-year-old male patient with bicuspid aortic valve. Systolic (upper row) and diastolic (lower row) frames from CS 4D flow reconstruction (Arterys). The left column is displayed on a bright blood background (note the high vascular signal due to the ferumoxytol) and the right column on a filtered black blood background. The posteriorly orientated, large aortic regurgitant jet is well-appreciated, as are the flow vectors throughout the arch and cardiac chambers. The regurgitation fraction was estimated at 43% both on 4D flow and 2D flow. (The exactness of the correspondence was surprising!)

is a therapeutic agent that is approved by the U.S. Food and Drug Administration for treatment of iron deficiency anemia in patients at all levels of renal function [12]. It is not approved for diagnostic applications and its use for MRI is off-label. Moreover, ferumoxytol has carried a boxed warning since March 2015. This concerns the risk of anaphylactic reactions, apparently linked to rapid administration during therapeutic use [13]. When used for MRI, ferumoxytol is normally infused slowly and in diluted form with close monitoring, and preliminary safety data on diagnostic use suggest an adverse event rate similar to the macrocyclic gadolinium agents [14]. Further data and analysis on the safety and diagnostic performance of ferumoxytol are needed, but the potential of the agent is clear when used appropriately.

Conclusion

In summary, we discussed the applications of 4D imaging in children and adult patients with congenital heart disease, illustrated with one example from each cohort. The combination of ferumoxytol and multi-dimensional MR imaging represents a powerful blend of MR technology and pharmacological contrast enhancement. The hope for the future is that, with more widespread availability of advanced multi-dimensional techniques and ferumoxytol enhancement, the true clinical potential of this approach will be realized in the broader community.

References

1 Han F, Zhou Z, Han E, Gao Y, Nguyen KL, Finn JP, et al. Self-gated 4D multiphase, steady-state imaging with contrast enhancement (MUSIC) using rotating cartesian K-space (ROCK): Validation in children with congenital heart disease. Magn Reson Med. 2017;78(2):472–483.

2 Zhou Z, Han F, Rapacchi S, Nguyen KL, Brunengraber DZ, Kim GJ, et al. Accelerated ferumoxytol-enhanced 4D multiphase, steady-state imaging with contrast enhancement (MUSIC) cardiovascular MRI: validation in pediatric congenital heart disease. NMR Biomed. 2017;30(1):10.1002/nbm.3663.

3 Han F, Zhou Z, Han E, Gao Y, Nguyen KL, Finn JP, et al. Self-gated 4D multiphase, steady-state imaging with contrast enhancement (MUSIC) using rotating cartesian K-space (ROCK): Validation in children with congenital heart disease. Magn Reson Med. 2017;78(2):472–483.

4 Di Sopra L, Piccini D, Coppo S, Stuber M, Yerly J. An automated approach to fully self-gated free-running cardiac and respiratory motion-resolved 5D whole-heart MRI. Magn Reson Med. 2019;82(6):2118–2132.

5 Roy CW, Di Sopra L, Whitehead KK, Piccini D, Yerly J, Heerfordt J, et al. Free-running cardiac and respiratory motion-resolved 5D whole-heart coronary cardiovascular magnetic resonance angiography in pediatric cardiac patients using ferumoxytol. J Cardiovasc Magn Reson. 2022;24(1):39.

6 Munoz C, Fotaki A, Botnar RM, Prieto C. Latest Advances in Image Acceleration: All Dimensions are Fair Game. J Magn Reson Imaging. 2023;57(2):387–402.

7 Falcão MBL, Di Sopra L, Ma L, Bacher M, Yerly J, Speier P, et al. Pilot tone navigation for respiratory and cardiac motion-resolved free-running 5D flow MRI. Magn Reson Med. 2022;87(2):718–732.

8 Han F, Rapacchi S, Khan S, Ayad I, Salusky I, Gabriel S, et al. Four-dimensional, multiphase, steady-state imaging with contrast enhancement (MUSIC) in the heart: a feasibility study in children. Magn Reson Med. 2015;74(4):1042–1049.

9 Nguyen KL, Han F, Zhou Z, Brunengraber DZ, Ayad I, Levi DS, et al. 4D MUSIC CMR: value-based imaging of neonates and infants with congenital heart disease. J Cardiovasc Magn Reson. 2017;19(1):40.

10 Nguyen KL, Ghosh RM, Griffin LM, Yoshida T, Bedayat A, Rigsby CK, et al. Four-dimensional Multiphase Steady-State MRI with Ferumoxytol Enhancement: Early Multicenter Feasibility in Pediatric Congenital Heart Disease. Radiology. 2021;300(1):162–173.

11 Mukai K, Burris NS, Mahadevan VS, Foster ED, Ordovas KG, Hope MD. 4D flow image quality with blood pool contrast: a comparison of gadofosveset trisodium and ferumoxytol. Int J Cardiovasc Imaging. 2018;34(2):273–279.

12 U.S. Food and Drug Administration. Feraheme Label. [cited February 5, 2018]; Available from: https://www.accessdata.fda.gov/drugsatfda_docs/label/2018/022180s009lbl.pdf

13 U.S. Food and Drug Administration. FDA Drug Safety Communication: FDA strengthens warnings and changes prescribing instructions to decrease the risk of serious allergic reactions with anemia drug Feraheme (ferumoxytol). 2015. [cited September 18, 2023]. Available from: http://www.fda.gov/Drugs/DrugSafety/ucm440138.htm

14 Nguyen KL, Yoshida T, Kathuria-Prakash N, Zaki IH, Varallyay CG, Semple SI, et al. Multicenter Safety and Practice for Off-Label Diagnostic Use of Ferumoxytol in MRI. Radiology. 2019;293(3):554–564.

Check out the movie files for all figures at
magnetomworld.siemens-healthineers.com/clinical-corner/case-studies/ferumoxytol

Contact

J. Paul Finn, M.D.
Department of Radiological Sciences
University of California Los Angeles
Peter V. Ueberroth Building, Suite 3371
10945 Le Conte Ave
Los Angeles, CA 90095-7206
USA
PFinn@mednet.ucla.edu

Clinical Value of Free-Breathing Cardiac Cine MRI with Compressed Sensing Real-Time Imaging and Retrospective Motion Correction

Masahiro Takakado[1], Yoshiaki Komori[2], Tomoyuki Kido[3]

[1]Department of Radiology, Ehime Prefectural Central Hospital, Ehime, Japan
[2]Siemens Healthcare K.K., Tokyo, Japan
[3]Department of Radiology, Ehime University Graduate School of Medicine, Ehime, Japan

Introduction

Comprehensive cardiac MRI is known as a method that enables the evaluation of a wide variety of parameters, such as morphology and function by cine MRI, myocardial ischemia by myocardial perfusion, myocardial fibrosis by late gadolinium enhancement (LGE), coronary artery stenosis by coronary artery MR angiography (MRA), and quantitative blood flow by phase-contrast sequences. However, the burden on patients due to the long examination time and the high threshold for clinical use are a major problem. A new free-breathing (FB) cardiac cine MR imaging technique using compressed sensing (CS) real-time imaging and retrospective motion correction has been developed (FB RTCS cine MoCo). This new cine MRI imaging technique is expected to shorten examination time and reduce the patient burden by eliminating the need for breath-hold (BH). This report reviews the new FB cine MRI technique and its clinical value.

1 Comparing conventional FB cine **(1A)** and FB RTCS cine MoCo **(1B)**. In conventional FB cine, the image is unclear and difficult to evaluate due to breathing artifacts. In FB RTCS cine MoCo, the motion correction technique produces a clear image even under free breathing.

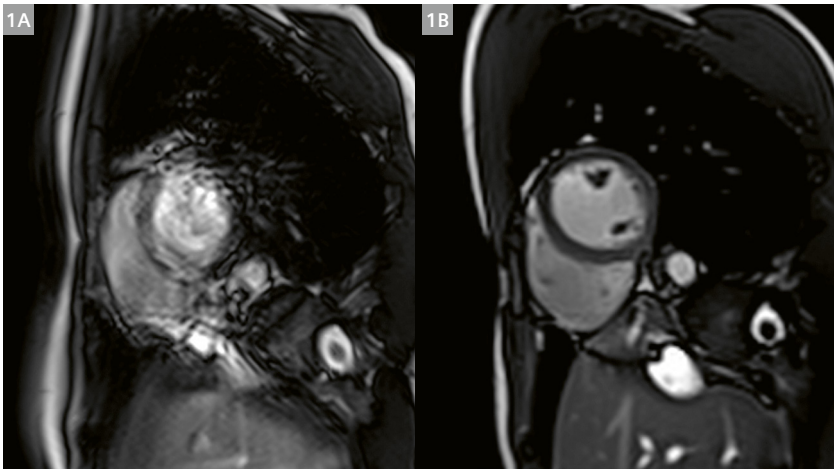

	Conventional BH cine	FB RTCS cine MoCo
Sequence type	2D cine bSSFP	2D cine bSSFP
Acceleration technique	GRAPPA	CS
TE/TR (ms)	1.4/3.2	1.4/3.2
Temporal resolution (ms)	40	43
FOV (mm)	360 × 360	360 × 360
Image matrix	192 × 125	192 × 125
Reconstructed spatial resolution (mm)	1.9 × 1.9	1.9 × 1.9
Slice thickness (mm)	6	6
No. of slices	12	12
Slice gap (mm)	4	4
Flip angle (degrees)	50	38
Bandwidth (Hz/pixel)	1302	1132
Cardiac phases	25	25
No. of BHs	6 or 12	–
Acceleration factor	3	12.5
Iterative reconstruction (n)	–	60

Table 1: **Imaging parameters of conventional BH cine and FB RTCS cine MoCo.**
(BH breath-hold, FB free-breathing, RT real-time, CS compressed sensing, MoCo motion correction, bSSFP balanced steady-state free-precession, GRAPPA generalized autocalibrating partially parallel acquisitions, TE echo time, TR repetition time, FOV field of view)

Cine MRI

Cardiac cine MRI is a routine part of every cardiac MRI. Based on cine images cardiac morphology and quantitative cardiac function can be evaluated. The latter is considered as gold standard due to its high reproducibility [1]. Compared to echocardiography, which is an important modality for cardiac functional assessment, cardiac cine MRI has the advantage of providing images without blind areas. Due to its anatomical and functional characteristics, cardiac cine MRI requires the control and management of both respiratory motion and cardiac motion and is generally performed under breath-hold (BH) to avoid respiratory motion artifacts. However, in conventional cine MRI using parallel imaging, only one to two slices of image data can be collected per BH, and multiple BHs are required to obtain images of the entire heart [2–3]. In addition, BH examinations require not only the cooperation of the patients and the time to collect data, but also the time for ancillary procedures such as breaks between BHs and BH announcements. Thus, the conventional BH cine MRI has been problematic due to prolonged examination time, increased patient burden, poor BH reproducibility, and poor image quality due to BH failure. A new FB cine MRI technique that combines CS real-time imaging and motion correction has been developed (FB RTCS cine MoCo) to address these issues. This technique is expected to shorten examination time and reduce patient burden through FB examination, and to improve image quality through motion correction. A detailed explanation of CS is beyond the scope of this report. Briefly, it is a technique for accelerating the reconstruction of high-quality images that are close to the original image from a small number of randomly sampled data [4], and its usefulness has already been widely recognized in clinical practice.

FB RTCS cine motion correction

In the following, we explain the data collection and reconstruction method of FB RTCS cine MoCo.

1 FB RTCS cine MoCo continuously collects data for multiple heartbeats per slice to ensure coverage of the end expiratory position. In this work, we set the acquisition duration to be 12 beats per slice. Considering that a typical respiratory cycle is about four seconds, this allows the end expiratory phase to be covered at least once for heart rates up to 180 bpm.

2 During image reconstruction, each heartbeat is normalized to the same number of cardiac phases (25 in this work) through *k*-space data rebinning. Then, the rebinned *k*-space data are sent for iterative reconstruction with spatio-temporal regularization. All heartbeats are jointly reconstructed.

3 Next, all acquired heartbeats are ranked by the amount of respiratory and other non-cardiac motion they contain. To do so, a motion score calculated for each heartbeat, defined as the sum of pixel-wise absolute difference between the first and last frames. Intuitively, the first and last frames should look almost identical absent of any respiratory or body motion, and hence the motion score is low. Otherwise, the two frames will be very different, and the motion score will be high.

4 With the heartbeats ranked, a subset (one third in this work) of highest ranked heartbeats are selected. In addition, heartbeat data during arrhythmia that deviates from the median RR interval by two standard deviations or more is automatically excluded. Finally, each accepted heartbeat is non-rigidly registered to the top-ranked heartbeat, and the registered heartbeats are averaged to form the final output.

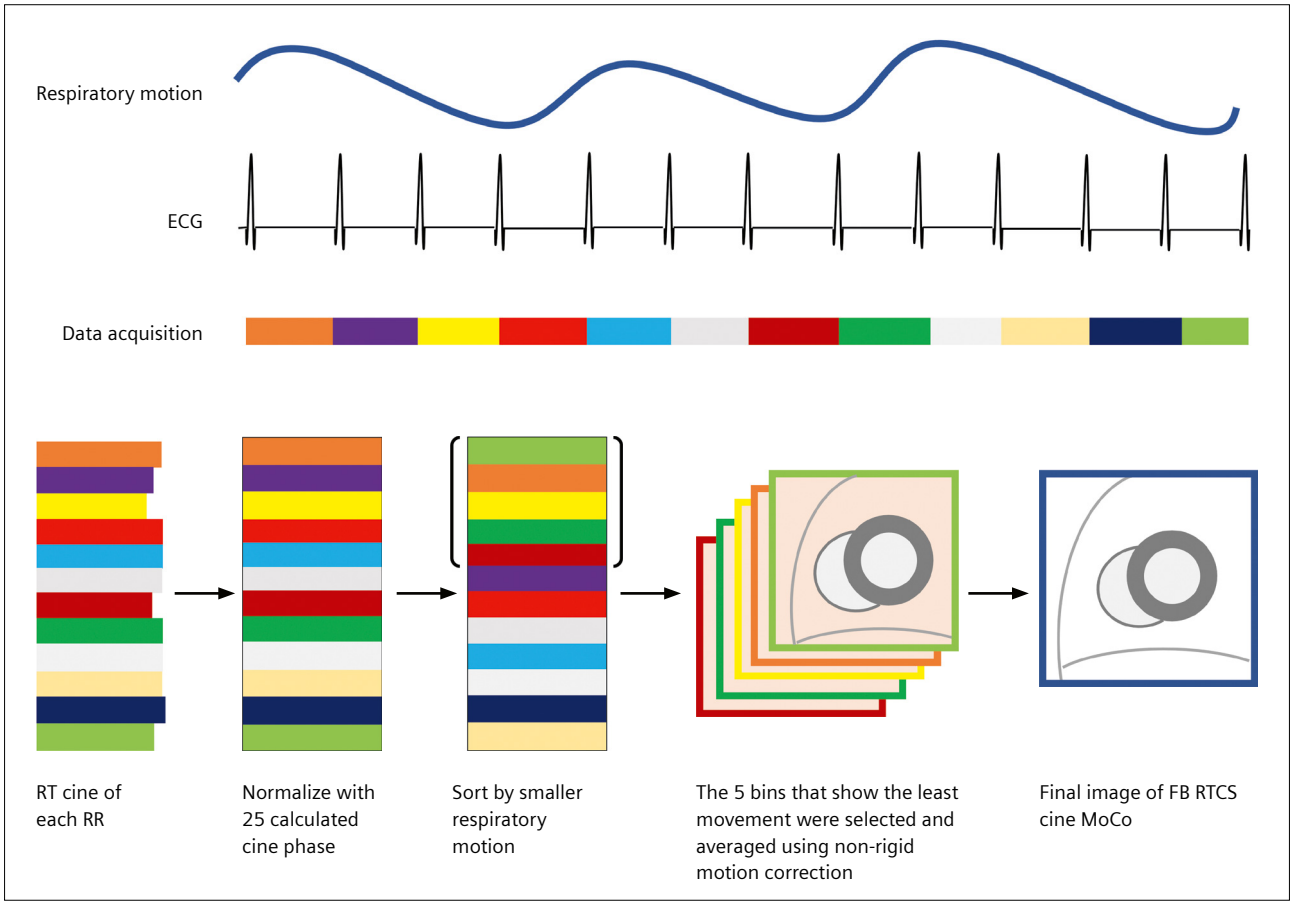

2 FB RTCS cine MoCo acquisition and reconstruction workflow.

In our initial study comparing conventional multiple BH cine with FB RTCS cine MoCo in healthy volunteers, there were no significant differences in either the assessment of both ventricular functions or the qualitative and quantitative image quality assessment, and the examination time was reduced [5]. Compared to a previous study of CS cine MRI under FB [6], FB RTCS cine MoCo improved image quality and reduced inter-examination error. The use of data from multiple heartbeats combined with motion correction may have been effective. Although cine MRI using similar motion correction techniques has been reported [7], the FB RTCS cine MoCo combined with CS has reduced examination time and improved clinical utility.

The advantage of FB RTCS cine MoCo is that the data used for reconstruction is selected by directly confirming the heart position, so the effect of respiration is minimized and high-quality images can be produced even in FB. The FB RTCS cine MoCo would also allow for improved spatial and temporal resolution imaging compared to single-shot FB CS cine without MoCo. In addition, FB RTCS cine MoCo is a continuous data acquisition technique, so the examination can be completed in 12 heartbeats multiplied by the number of slices. Thus, FB RTCS cine MoCo may be suitable for cardiac hypertrophy cases because an additional slice does not significantly prolong the examination time. Although this technique is applicable to all patients, thanks to the reduced burden due to the elimination of BH, it is expected to be particularly useful for the elderly, patients in poor condition, children, and patients under sedation, who have difficulty holding their breath.

Conclusion

In the future, it would be ideal to complete all cardiac MRI sequences under FB. The patient would only have to get on the table and the examination could be completed while the patient is sleeping. This would greatly reduce the burden of the examination and increase the usefulness of MRI as one of the routine cardiac examinations. Recently, new technologies such as FB coronary MRA using CS [8] and FB 3D LGE combined with CS and navigation images [9] have also been reported. It is expected that the shortening of each sequence will improve the overall examination workflow.

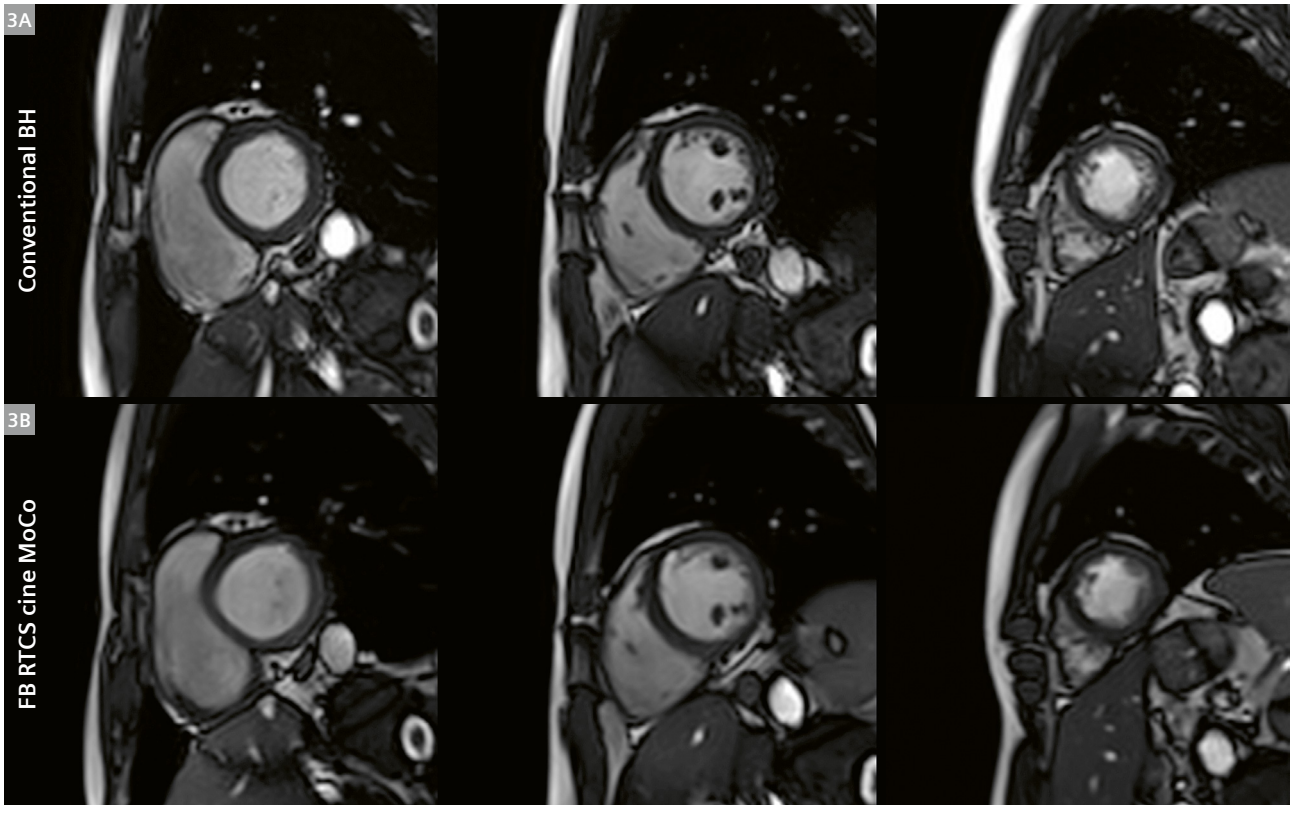

3 Comparison of representative short-axis cine images in end-diastole. Conventional BH cine **(3A)** and FB RTCS cine MoCo **(3B)**.

References

1 Greupner J, Zimmermann E, Grohmann A, Dübel HP, Althoff TF, Borges AC, et al. Head-to-head comparison of left ventricular function assessment with 64-row computed tomography, biplane left cineventriculography, and both 2- and 3-dimensional transthoracic echocardiography: comparison with magnetic resonance imaging as the reference standard. J Am Coll Cardiol. 2012;59(21):1897-907. Erratum in: J Am Coll Cardiol. 2012;60(5):481.

2 Kozerke S, Plein S. Accelerated CMR using zonal, parallel and prior knowledge driven imaging methods. J Cardiovasc Magn Reson. 2008;10(1):29.

3 Xu J, Kim D, Otazo R, Srichai MB, Lim RP, Axel L, et al. Towards a five-minute comprehensive cardiac MR examination using highly accelerated parallel imaging with a 32-element coil array: feasibility and initial comparative evaluation. J Magn Reson Imaging. 2013;38(1):180-8.

4 Candes E, Romberg J, Tao T. Robust uncertainty principles: Exact signal reconstruction from highly incomplete frequency information. IEEE Trans Inf Theory. 2006;52(2):489-509.

5 Takakado M, Kido T, Ogawa R, Takimoto Y, Tokuda T, Tanabe Y, et al. Free-breathing cardiovascular cine magnetic resonance imaging using compressed-sensing and retrospective motion correction: accurate assessment of biventricular volume at 3T. Jpn J Radiol. 2023;41(2):142-152.

6 Kido T, Kido T, Nakamura M, Watanabe K, Schmidt M, Forman C, et al. Assessment of Left Ventricular Function and Mass on Free-Breathing Compressed Sensing Real-Time Cine Imaging. Circ J. 2017;81(10):1463-1468.

7 Rahsepar AA, Saybasili H, Ghasemiesfe A, Dolan RS, Shehata ML, Botelho MP, et al. Motion-Corrected Real-Time Cine Magnetic Resonance Imaging of the Heart: Initial Clinical Experience. Invest Radiol. 2018;53(1):35-44.

8 Hirai K, Kido T, Kido T, Ogawa R, Tanabe Y, Nakamura M, et al. Feasibility of contrast-enhanced coronary artery magnetic resonance angiography using compressed sensing. J Cardiovasc Magn Reson. 2020 Feb 13;22(1):15.

9 Zeilinger MG, Wiesmüller M, Forman C, Schmidt M, Munoz C, Piccini D, et al. 3D Dixon water-fat LGE imaging with image navigator and compressed sensing in cardiac MRI. Eur Radiol. 2021;31(6):3951-3961.

Contact

Masahiro Takakado, M.D.
Ehime Prefectural Central Hospital
Department of Radiology
83, Kasugamachi, Matsuyama, Ehime
Japan
Tel.: +81-89-947-1111
takakado.masahiro.uf@ehime-u.ac.jp

3D Whole-Heart Imaging: An Innovative Collaborative Solution

Karl P. Kunze[1,2], Jens Wetzl[3], Seung Su Yoon[3], Radhouene Neji[2], Gaia Banks[3], Rene Botnar[2,4,5], Claudia Prieto[2,4], Michaela Schmidt[3]

[1]MR Research Collaborations, Siemens Healthcare Limited, Camberley, United Kingdom
[2]School of Biomedical Engineering and Imaging Sciences, King's College London, United Kingdom
[3]Cardiovascular MR Predevelopment, Siemens Healthcare GmbH, Erlangen, Germany
[4]Escuela de Ingeniería, Pontificia Universidad Católica de Chile, Santiago, Chile
[5]Institute for Biological and Medical Engineering, Pontificia Universidad Católica de Chile, Santiago, Chile

Clinical need

A broad spectrum of clinical use cases for cardiovascular magnetic resonance imaging (CMR) profit from high isotropic resolution in three dimensions to show thoracic vasculature including the small and tortious coronary artery vessels and fibrosis/myocardial viability using the late gadolinium enhancement (LGE) measurement technique. Recent clinical studies have demonstrated the value of free-breathing, high-isotropic-resolution CMR to diagnose ischemic heart disease using coronary artery and vein [1, 2] or LGE imaging [3], cardiomyopathy [4], congenital [5] and structural [6] heart disease, and ablation lesion assessment [7].

Challenges

One challenge of using a high isotropic resolution in the range of 1 mm^3 to 1.3 mm^3 in the context of CMR exams is the prolonged scan time when compared to other imaging methods. Although CMR has several benefits including high tissue contrast and no need for radiation, it remains a comparatively slow imaging modality. For whole-heart coverage with high isotropic resolution, a novel imaging strategy is required to complete scans in 5 to 10 minutes.

Ideally, these measurements should be acquired in free breathing. Hence, cardiac and respiratory motion must be addressed. To minimize cardiac motion, scanning should be performed during a time in the cardiac cycle when the heart is in its quiescent phase, usually at end-diastole with a window of 80–160 ms, depending on the heart rate. To find the still phase of the heart, a 4-chamber cine is usually acquired. An experienced operator needs to manually define it and then enter it correctly in the 3D measurement protocol.

To account for respiratory motion, navigators are typically used to scan during free breathing. The frequently used 1D cross-paired diaphragm navigators are manually placed on the liver dome, and imaging data are accepted only in end-expiration. Depending on the breathing pattern, the acceptance rate can be between 20% and 60%. Therefore, scan time is unpredictable upfront, and a drift in breathing pattern during the scan may further decrease acquisition efficiency.

Moreover, accepting data only in end-diastole and in end-expiration makes data sampling very inefficient. Long scan times result in high institutional costs and are a discomfort for sick patients, meaning they can result in patient movement (reduced patient compliance) and non-diagnostic images.

One method to overcome this hurdle is the "free-running" acquisition approach, which samples and uses all data irrespective of the breathing and cardiac-motion states, with separation of these during image reconstruction [8, 9]. While this single-click method has numerous benefits that have been shown in multiple publications, it has not yet been widely distributed and tested clinically because it requires high-end computing, long reconstruction times, and often the use of contrast agent.

Another way to account for respiratory motion is to use image-based navigators [10] combined with non-rigid motion-compensated reconstruction. This enables predictable scan times and an acceptance rate of 100% of data irrespective of the breathing position. When combined with novel undersampling strategies [11, 12], a scan time of 5 to 8 minutes is possible, while the reconstruction only needs to address respiratory-motion compensation and *k*-space undersampling.

3D Whole Heart is work in progress. The application is currently under development and is not for sale in the U.S. and in other countries. Its future availability cannot be ensured.

A third challenge for 3D imaging is the workflow, including positioning of multiple objects like navigators, saturation bands, and imaging volume, and determining the appropriate resting phase in the cardiac cycle as mentioned above. For the LGE measurements, correctly estimating inversion time (TI) to null healthy myocardium is yet another task for operators.

Finally, robust fat saturation is key for high-contrast display of the coronary arteries, as they are embedded in epicardial fat. For certain LGE applications, the separation of fat and water is also essential, e.g., in patients with pericarditis or small endomyocardial fibrosis, where it can be difficult to distinguish between fat and lesion.

The solution

To overcome the limitations of 1D diaphragmatic navigators, 2D image navigators (iNAV) have been proposed to enable direct tracking of the impact of respiratory motion on the heart [9]. With iNAV imaging, it is possible to derive accurate quantitative motion information in two spatial dimensions. This enables retrospective motion correction rather than prospective gating, resulting in 100% respiratory scan efficiency and predictable scan times.

While iNAV imaging allows for direct correction of beat-to-beat translational respiratory motion in a predefined image region, accounting for non-rigid motion during the breathing cycle requires a more complex, non-rigid motion-compensated reconstruction framework. A first step in such approaches is often data binning, followed by reconstruction of different bin images representing the different respiratory motion states present in the data. As each bin image only contains a small fraction of the already undersampled 3D acquisition, reconstruction of the individual bin images requires a well-designed interplay of acquisition patterns and reconstruction algorithms.

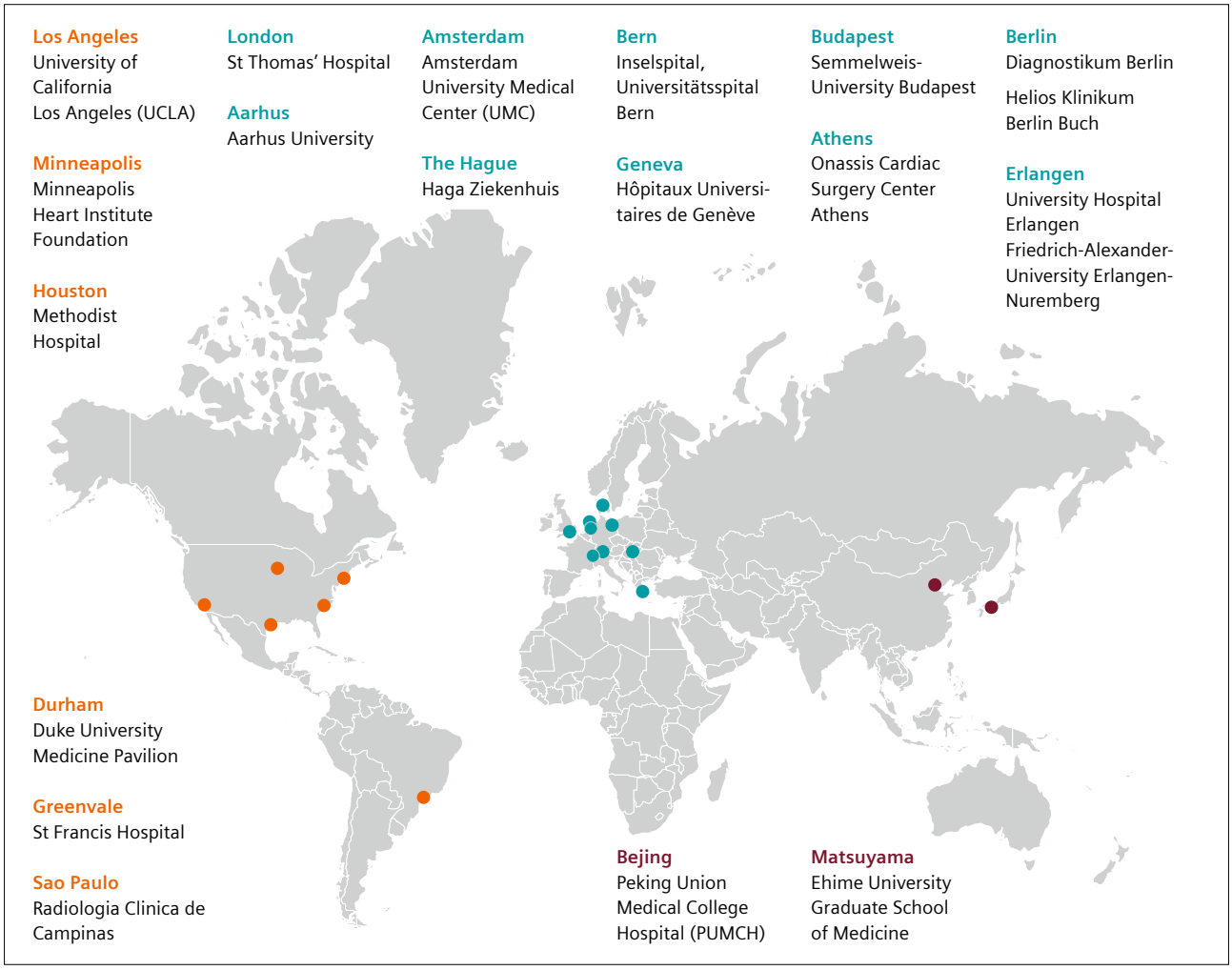

1 **Clinical partners for validating the 3D Whole-Heart application**
Our clinical partners helped us by sharing their experience so we could improve the research sequence and make it robust for a wide range of clinical questions and settings.

The variable-density Cartesian trajectory with spiral profile order sampling (VD-CASPR) [11, 12] provides high overall undersampling factors while maintaining favorable undersampling properties when data is split up into respiratory bins, enabling regularized reconstruction of artifact-free respiratory bin images [13]. These bin images can then be used to estimate 3D non-rigid motion between the motion states they represent, and motion information can be used in a final, non-rigid motion-compensated reconstruction of all data [14, 15]. Despite the large number of steps involved, the computational burden in the form of reconstruction time can be minimized to orders of 1 to 2 minutes using implementations with modern GPU technology [16].

In addition to standard chemical shift-based fat saturation methods, the described approach can be combined with Dixon-based fat-water separation. This provides a means to achieve robust elimination of fat from the final water-only image [17, 18], while also providing a fat-only image that can enable, e.g., discrimination between bright myocardial scar signal and fatty infiltration (Figure 2). Dixon fat-water separation enables improved visualisation of the coronary arteries [18], especially at 3T.

Workflow automation

As previously described, whole-heart imaging has typically increased the workload and requires more experienced operators given the need for precise positioning of saturation bands, image navigator, resting phase, and potentially TI. Together with the novel whole-heart sequence, we now offer workflow support for many of the planning steps that previously required manual user input.

In the following, we describe three modules for automating common planning tasks: AutoPositioning (for placement of graphical objects, e.g., the imaging volume, navigator, saturation bands) [19]; AutoRestingPhase (to determine a suitable acquisition window during the quiescent period in the cardiac cycle) [20]; and AutoTI (to set the proper inversion time for subsequent LGE imaging) [21].

AutoPositioning is based on localizer scans in coronal and transversal orientations. It uses deep learning to detect multiple anatomical structures, including the location and size of the heart and left ventricle, as well as the location of the liver dome and the arms. These are used to automatically perform the subsequent planning steps. Based on an initial localizer, the heart is placed into the isocenter, and further localizers centered on the heart can be acquired. Slices for thorax overview imaging and the AutoAlign scout can be positioned. For the whole-heart sequence, the imaging volume including slice coverage and position of the image navigator and saturation bands can be set automatically.

AutoRestingPhase is based on a 4-chamber-view cine to determine the quiescent phases of different cardiac structures within the cardiac cycle. First, the right coronary artery (RCA) and the four chambers of the heart are automatically detected. Subsequently, their motion throughout the cardiac cycle is tracked via image registration and then quantified and displayed as a motion curve. The valleys in this motion curve serve as suggestions for the whole-heart acquisition window. Different types of whole-heart acquisition can use the resting phase results of different anatomies of interest, e.g., the RCA for T2-prepared angiography or the left ventricle for 3D LGE.

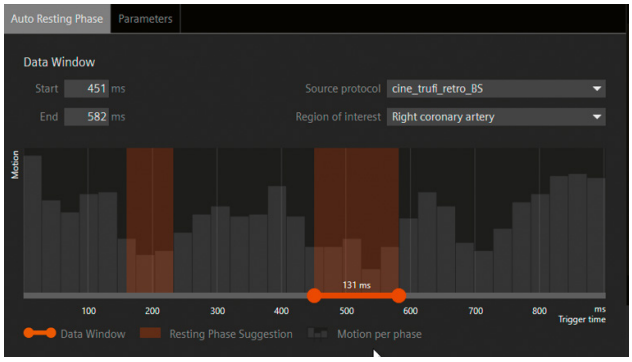

AutoTI is based on a TI scout in short-axis orientation, which is segmented to find the myocardial and blood-pool intensity values at each inversion time. The minimum of the myocardial intensity curve is first used to determine a TI with optimal myocardial nulling, then refined by finding an adjacent TI time with improved blood-myocardium contrast in case both have their zero crossings at similar times. An offset can then be applied automatically to subsequent LGE acquisitions to account for the time between TI scout and LGE acquisitions. This is applicable both to conventional 2D LGE and the novel 3D LGE acquisition.

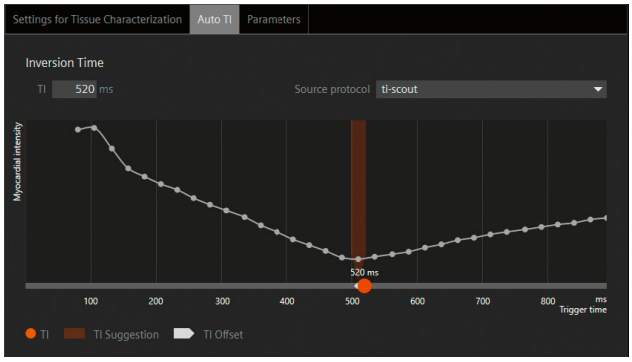

The combination of these modules significantly reduces the complexity and workload involved in performing high-quality whole-heart acquisitions, and simplifies or even improves the entire scan workflow.

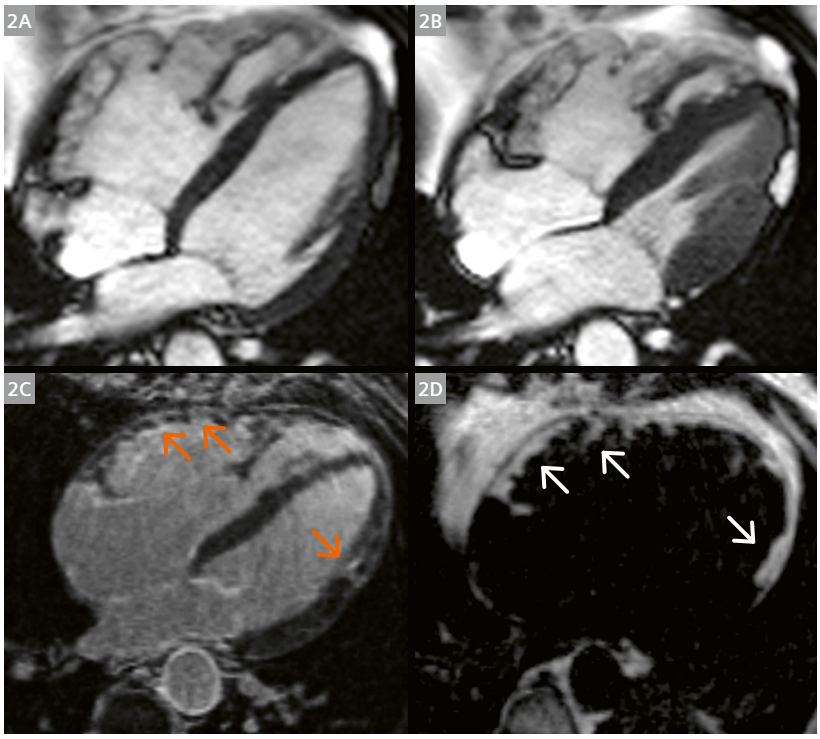

2 A 60-year-old male patient with fibrofatty replacement in LGE of the free wall of the RV and LV. Cine imaging 4-chamber view in a diastolic phase **(2A)** and systolic phase **(2B)**. The 3D whole-heart technique allows a differentiation between fibrosis **(2C)** in water-only LGE images and fat deposits **(2D)** in fat-only images. Fat deposition is depicted by the white arrows. Fibrosis is depicted by the orange arrows.
CMR imaging was performed on a 1.5 Tesla scanner (MAGNETOM Avanto fit, Siemens Healthcare, Erlangen, Germany) using cine imaging steady-state free precession (SSFP). After application of gadolinium-based contrast media (gadoteridol 0.2 mmol/kg), image-based navigated 3D whole-heart LGE sequence with fat–water separation was performed.
Images courtesy of Edyta Blaszczyk, MD[1,2,3], and Jeanette Schulz-Menger, MD[1,2,3,4]

[1]Charité – Universitätsmedizin Berlin, corporate member of Freie Universität Berlin and Humboldt-Universität zu Berlin, ECRC Experimental and Clinical Research Center, Berlin, Germany. [2]Working Group on Cardiovascular Magnetic Resonance, Experimental and Clinical Research Center, a joint cooperation between Charité Medical Faculty and the Max-Delbrück Center for Molecular Medicine. [3]DZHK (German Centre for Cardiovascular Research), partner site Berlin, Germany. [4]HELIOS Hospital Berlin-Buch, Department of Cardiology and Nephrology, Berlin, Germany.

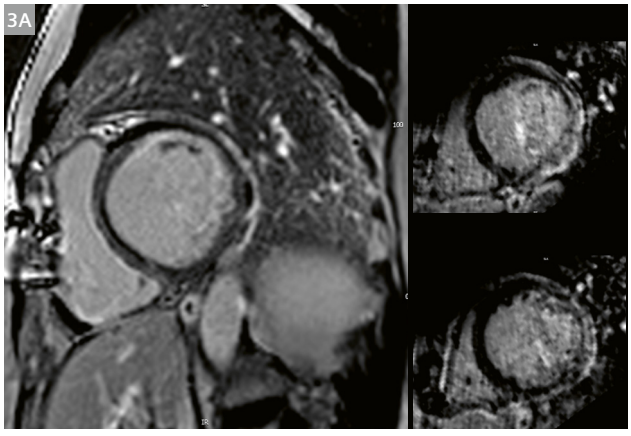

3 53-year-old male patient. **(3A)** Sustained VTs, MVR (MVP), DCM like phenotype of HF. **(3B)** Identify potential ablation targets from 3D corridors of border zone tissue and verify the detected corridors directly with the DICOM images. **(3C)** Import pre-procedural imaging into any electroanatomic mapping (EAM) system. Agreement of the structural arrhythmogenic substrate detected as corridors by CMR 3D LGE and the sites of electrical channels that may serve as the isthmus of VT. Late potentials and local abnormal ventricular activities at the areas of structural VT corridors.
CMR imaging was performed on a 1.5 Tesla MAGNETOM Sola (Siemens Healthcare, Erlangen, Germany).
Images courtesy of Evangelia Nyktari, M.D. (CMR); Athanasios Saplaouras, M.D. (EP lab); Konstantinos Letsas, M.D., Ph.D. (EP lab); Michalis Efremidis, M.D., Ph.D. (EP Lab); P Rozos and S Zarkadoulas (CMR) at Onassis Cardiac Surgery Center, Athens, Greece.

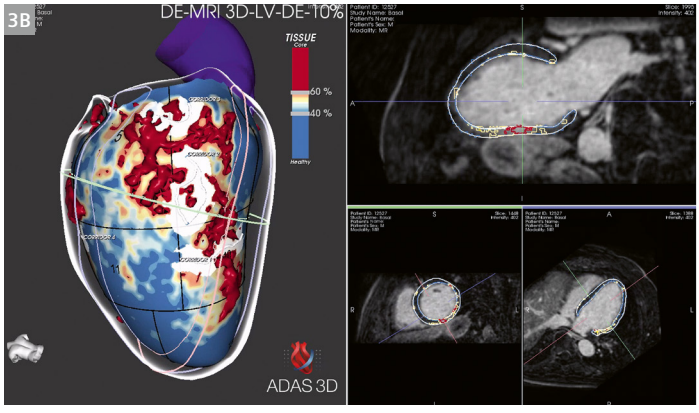

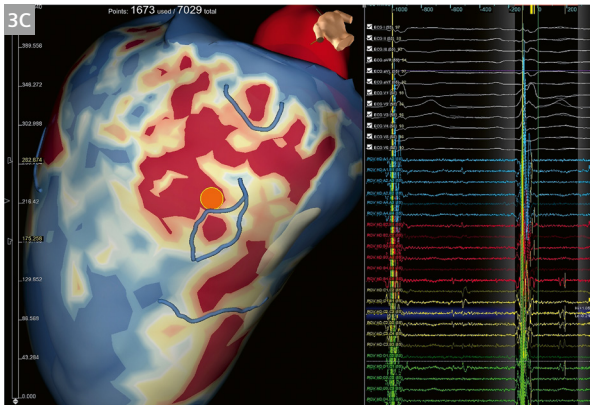

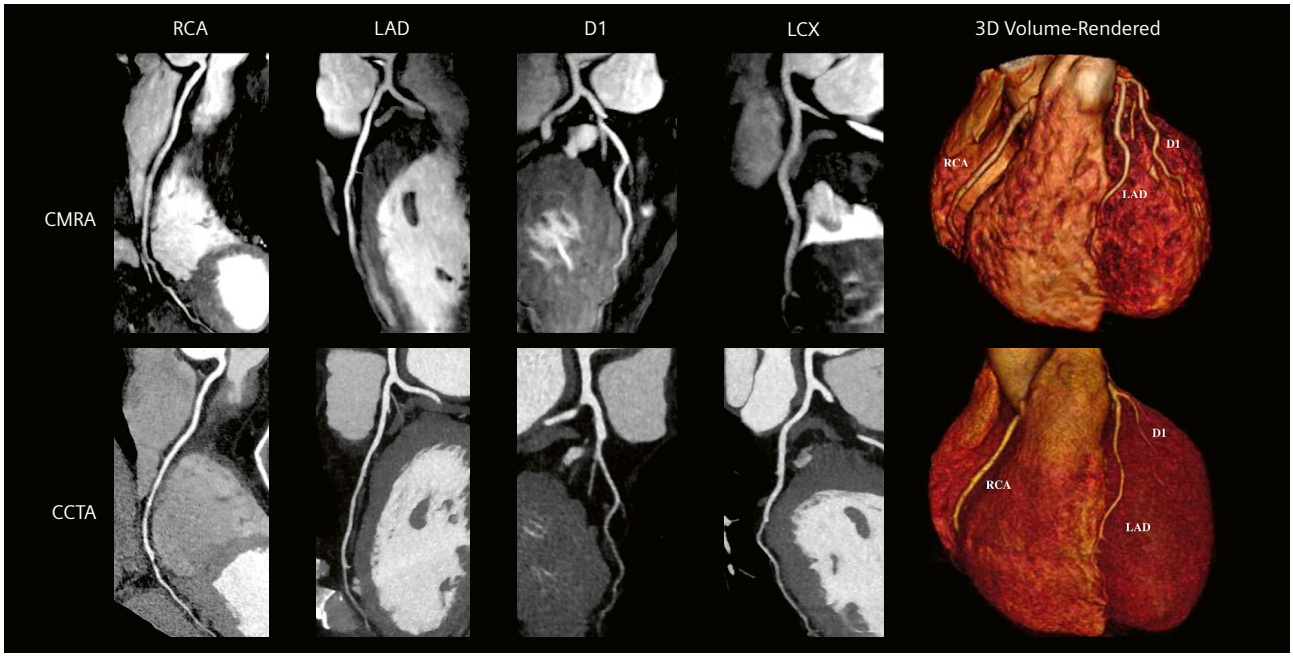

4 Curved multiplanar reformat and 3D volume-rendered non-contrast CMRA and contrast-enhanced CCTA in a 54-year-old male with no significant stenosis.
Abbreviations: CMRA = coronary magnetic resonance angiography; CCTA = coronary computed tomography angiography; RCA = right coronary artery; LAD = left anterior descending artery; D1 = first diagonal artery; LCX = left circumflex artery.
CMR imaging was performed on a 1.5 Tesla MAGNETOM Aera (Siemens Healthcare, Erlangen, Germany).
Images courtesy of Reza Hajhosseiny, M.D.[1]; Aurélien Bustin, Ph.D.[1]; Imran Rashid, M.D., Ph.D., FRACP[1]; Gastao Cruz, Ph.D.[1]; Ronak Rajani, M.D., Ph.D., FACC, FRCP[2]; Claudia Prieto, Ph.D.[1]; René M. Botnar, Ph.D.[1]; et al.
Adapted and reproduced from Hajhosseiny et al. [22].

[1]*School of Biomedical Engineering and Imaging Sciences, King's College London, United Kingdom*
[2]*School of Cardiovascular Medicine and Sciences, King's College London, United Kingdom*

Technical partner for developing the 3D Whole-Heart application

The whole-heart imaging sequence, image navigator, and image reconstruction framework described here were developed in close collaboration with the research groups of Professor René Botnar and Professor Claudia Prieto at King's College London, UK.

Conclusion and outlook

Clinical validation, resp. research studies, and feedback from numerous global sites indicate that implementing the novel 3D Whole-Heart sequence from Siemens Healthineers makes scans with whole-heart coverage and high isotropic resolution routinely possible in 5 to 10 minutes. Given the high level of automation available to support operators and achieve faster scan times, we expect rapid clinical adoption.

References

1 Hajhosseiny R, Rashid I, Bustin A, Munoz C, Cruz G, Nazir MS, et al. Clinical comparison of sub-mm high-resolution non-contrast coronary CMR angiography against coronary CT angiography in patients with low-intermediate risk of coronary artery disease: a single center trial. J Cardiovasc Magn Reson. 2021;23(1):57.
2 Nazir MS, Bustin A, Hajhosseiny R, Yazdani M, Ryan M, Vergani V, et al. High-resolution non-contrast free-breathing coronary cardiovascular magnetic resonance angiography for detection of coronary artery disease: validation against invasive coronary angiography. J Cardiovasc Magn Reson. 2022;24(1):26.
3 Peters AA, Wagner B, Spano G, Haupt F, Ebner L, Kunze KP, et al. Myocardial scar detection in free-breathing Dixon-based fat- and water-separated 3D inversion recovery late-gadolinium enhancement whole heart MRI. Int J Cardiovasc Imaging. 2023;39(1):135-144
4 Bustin A, Hua A, Milotta G, Jaubert O, Hajhosseiny R, Ismail TF, et al. High-Spatial-Resolution 3D Whole-Heart MRI T2 Mapping for Assessment of Myocarditis. Radiology. 2021;298(3):578-586.
5 Fotaki A, Pushparajah K, Hajhosseiny R, Schneider A, Alam H, Ferreira J, et al. Free-breathing, Contrast Agent-free Whole-Heart MTC-BOOST Imaging: Single-Center Validation Study in Adult Congenital Heart Disease. Radiol Cardiothorac Imaging. 2023;5(1):e220146.

6 Toupin S, Pezel T, Bustin A, Cochet H. Whole-Heart High-Resolution Late Gadolinium Enhancement: Techniques and Clinical Applications. J Magn Reson Imaging. 2022;55(4):967-987.
7 Sim I, Razeghi O, Karim R, Chubb H, Whitaker J, O'Neill L, et al. Reproducibility of Atrial Fibrosis Assessment Using CMR Imaging and an Open Source Platform. JACC Cardiovasc Imaging. 2019;12(10):2076-2077.
8 Di Sopra L, Piccini D, Coppo S, Stuber M, Yerly J. An automated approach to fully self-gated free-running cardiac and respiratory motion-resolved 5D whole-heart MRI. Magn Reson Med. 2019;82(6):2118-2132.
9 Roy CW, Di Sopra L, Whitehead KK, Piccini D, Yerly J, Heerfordt J, et al. Free-running cardiac and respiratory motion-resolved 5D whole-heart coronary cardiovascular magnetic resonance angiography in pediatric cardiac patients using ferumoxytol. J Cardiovasc Magn Reson. 2022;24(1):39.
10 Henningsson M, Koken P, Stehning C, Razavi R, Prieto C, Botnar RM. Whole-heart coronary MR angiography with 2D self-navigated image reconstruction. Magn Reson Med. 2012;67(2):437-445.
11 Prieto C, Doneva M, Usman M, Henningsson M, Greil G, Schaeffter T, et al. Highly efficient respiratory motion compensated free-breathing coronary MRA using golden-step Cartesian acquisition. J Magn Reson Imaging. 2015;41(3):738-746.

Contact

Michaela Schmidt
Siemens Healthineers
SHS DI MR RCT CLS CARD
Allee am Roethelheimpark 2
91050 Erlangen
Germany
michaela.schmidt@siemens-healthineers.com

Karl P. Kunze, Ph.D.
Siemens Healthineers
SHS EMEA GBI DI PI
Riverside Way
Camberley GU15 3YL
United Kingdom
karl-philipp.kunze@siemens-healthineers.com

12 Bustin A, Rashid I, Cruz G, Hajhosseiny R, Correia T, Neji R, et al. 3D whole-heart isotropic sub-millimeter resolution coronary magnetic resonance angiography with non-rigid motion-compensated PROST. J Cardiovasc Magn Reson. 2020;22(1):24.
13 Correia T, Ginami G, Cruz G, Neji R, Rashid I, Botnar RM, et al. Optimized respiratory-resolved motion-compensated 3D Cartesian coronary MR angiography. Magn Reson Med. 2018;80(6):2618-2629.
14 Batchelor PG, Atkinson D, Irarrazaval P, Hill DL, Hajnal J, Larkman D. Matrix description of general motion correction applied to multishot images. Magn Reson Med. 2005;54(5):1273-1280.
15 Cruz G, Atkinson D, Henningsson M, Botnar RM, Prieto C. Highly efficient nonrigid motion-corrected 3D whole-heart coronary vessel wall imaging. Magn Reson Med. 2017;77(5):1894-1908.
16 Zeilinger MG, Kunze KP, Munoz C, Neji R, Schmidt M, Croisille P, et al. Non-rigid motion-corrected free-breathing 3D myocardial Dixon LGE imaging in a clinical setting. Eur Radiol. 2022;32(7):4340-4351.
17 Munoz C, Cruz G, Neji R, Botnar RM, Prieto C. Motion corrected water/fat whole-heart coronary MR angiography with 100% respiratory efficiency. Magn Reson Med. 2019;82(2):732-742.
18 Munoz C, Bustin A, Neji R, Kunze KP, Forman C, Schmidt M, et al. Motion-corrected 3D whole-heart water-fat high-resolution late gadolinium enhancement cardiovascular magnetic resonance imaging. J Cardiovasc Magn Reson. 2020;22(1):53.
19 Wetzl J, Yoon S, Schmidt M, Haenel A-B, Weißgerber A, Barkhausen J, et al. AI-based Single-Click Cardiac MRI Exam: Initial Clinical Experience and Evaluation in 44 Patients. International Society for Magnetic Resonance in Medicine 2023.
20 Yoon S, Preuhs E, Schmidt M, Forman C, Chitiboi T, Sharma P, et al. Automated Cardiac Resting Phase Detection Targeted on the Right Coronary Artery. Machine Learning for Biomedical Imaging. 2023;2,arXiv:2109.02342:1-26.
21 Yoon S, Schmidt M, Rick M, Chitiboi T, Sharma P, Emrich T, et al. Validation of a deep learning based automated myocardial inversion time selection for late gadolinium enhancement imaging in a prospective study. International Society for Magnetic Resonance in Medicine 2021.
22 Hajhosseiny R, Rashid I, Bustin A, Munoz C, Cruz G, Nazir M.S, et al. Clinical comparison of sub-mm high-resolution non-contrast coronary MRA against coronary CTA in patients with low-intermediate risk of CAD: A single center trial. J Cardiovasc Magn Reson. 2021;23(1):57.

Artificial Intelligence: Learning About the Future of Cardiovascular MR

Kerstin Hammernik, Ph.D.[1] and Thomas Küstner, Ph.D.[2]

[1]Technical University of Munich, Germany / Imperial College London, UK
[2]University Hospital Tübingen, Germany

Over the past 40 years, cardiovascular magnetic resonance (CMR) has evolved from an esoteric research tool to an indispensable clinical tool that routinely changes patient management across the breadth of modern cardiovascular practice. CMR is a versatile, non-invasive imaging modality that provides a comprehensive assessment of multiple parameters for cardiac function and morphology in a single protocol. It plays a major role in the diagnosis and management of cardiovascular disease (CVD). The prevalence of CVD is increasing annually and the conditions are among the leading causes of morbidity and mortality worldwide. This requires improvements in assessing, diagnosing, treating, and monitoring CVD patients. CMR will play a central role in achieving these goals. However, there remain major challenges for the widespread use of this technique:

(a) Complex technology with many pulse sequences and parameters to choose from
(b) Manual data analysis and interpretation
(c) Inherent cardiac and respiratory motion
(d) Duration of the examination

Methods using artificial intelligence (AI) have been proposed to address these challenges, but have also given rise to new questions about the methods' reliability, accuracy, generalizability, and robustness. In order to shape the future of CMR and establish where and how AI can play a role in it, we will showcase some CMR applications and scenarios that reflect the abovementioned challenges. We will highlight some AI methods for each step of the CMR processing chain and conclude with thoughts on remaining challenges and opportunities.

Learning about the heart in higher dimensions

CMR enables the acquisition of morphological, functional, and quantitative tissue parameters. Various sequences are devised that represent powerful tools for the non-invasive characterization of congenital or acquired CVDs, including ischemia, valvular diseases, and ischemic and non-ischemic cardiomyopathies. Cardiac function is commonly assessed with continuous acquisitions (cine, real-time) over multiple cardiac cycles. Perfusion imaging permits the assessment of physiologic and pathophysiologic functional parameters. First-pass perfusion is the clinical standard for measuring myocardial blood flow and detecting myocardial ischemia. Cardiac viability is traditionally studied with a gadolinium-based contrast agent in late gadolinium enhancement. Cardiovascular flow by phase-contrast imaging measures the velocity of blood in the cardiac chambers and great vessels. Coronary magnetic resonance angiography (CMRA) has the potential to diagnose coronary artery diseases. Quantitative CMR techniques like T1, T2, or T1rho mapping provide characterization of tissue properties that distinguish healthy from diseased tissue. More recently, MR fingerprinting[1] and MR multitasking have been proposed to provide multi-parametric data in a continuously measured acquisition under a free-movement scenario (with respiration and a beating heart). Multi-parametric CMR offers the promise of a more accurate diagnosis, early disease detection, and monitoring over time or of response to therapy [1].

These applications require either high spatial and/or temporal resolution, should ideally be acquired in 3D with whole-heart coverage to avoid slice misalignments or to allow reformatting into arbitrary image orientations, or are susceptible to cardiac and respiratory motion. The achievable image quality must be sufficient to detect and characterize CVDs, and is thus an inherent trade-off between imaging resolution, scan time, and signal-to-noise ratio (SNR), which are overall challenging requirements to meet. Moreover, to fully utilize the available information and/or to resolve the individual factors (motion, relaxivity, perfusion, etc.), joint data processing of all acquired data should be performed. This in turn yields high-dimensional data processing for CMR. To give an example, 5D cine imaging provides 3D spatial information of respiratory (1D) and cardiac (1D) motion-resolved data. If we jointly reconstruct motion-resolved data, we can share spatiotemporal information, i.e., sharing samples at a spatial location

[1]*MR Fingerprinting is not commercially available in some countries. Due to regulatory reasons its future availability cannot be ensured.*

between different respiratory/cardiac motion states by accounting for the underlying motion between motion states. The benefit is increased sampling efficiency and higher sampling density, which in turn can result in improved image quality. Furthermore, high-dimensional data processing naturally lends itself to the combination of several data processing steps, as shown in Figure 1. In our 5D cine example, the image reconstruction is combined with a motion correction/estimation procedure. The combination could also expand across several processing steps and we could develop a single AI network that performs this task for us. Let us say we are actually interested in assessing the left ventricular function using the 5D cine imaging. We could thus combine reconstruction, motion estimation, and image segmentation (to obtain left ventricular functional parameters) using as input the acquired MR raw data and outputting the left ventricular functional parameters (ejection fraction, end-systolic volume, and so on). While joint processing has its benefits, one could also be interested in obtaining the intermediate results of this joint processing chain – to perform quality assurance, for instance, or to further visually assess morphology and function. However, depending on the selected setup, architecture, and scenario, this may no longer be easily possible. On the other hand, we could have developed individual and finely tuned AI networks for each of the tasks. For the 5D cine example, an image reconstruction network is followed by an image registration network that merges individually reconstructed motion states on which a subsequent image segmentation network is performed. Intermediate results (reconstructed image, motion fields, segmentation masks) would be available, but we would lose the possibility to share information between and within processing steps.

While the concepts of joint processing sound intriguing and have already been studied in several research settings, applying them to a clinical scenario in a reliable fashion is challenging. Furthermore, high-dimensional AI-based data processing is not trivial and currently still limited in most cases by the available graphics processing unit (GPU) memory and the availability of network building blocks to process data beyond 3D [2].

AI forming the CMR workflow

For a conventional CMR examination, several individual sequences are acquired, for which different processing steps are conducted. These include image acquisition, image formation, and diagnosis, as illustrated in Figure 1. These processing steps could be performed individually with highly optimized and tuned AI networks, or several steps could be combined end-to-end for outputting multiple results in so-called multi-tasking networks. While AI has the potential to improve each step of the imaging pipeline, it should be seen as a support for clinicians, not a replacement.

Scanning and planning

The most tedious and time-consuming part of CMR is planning the cardiac scan. The image quality depends on the experienced technician responsible for acquiring the data, and uncertainties might be introduced by incorrect planning. AI has the potential to speed up the whole planning workflow, resulting in increased patient comfort and reduced healthcare costs. Also, AI-supported planning allows for more standardized cardiac scans and reduces the complexity of cardiac view planning. Siemens Healthineers provides a solution for AI-based view planning with its myExam Cardiac Assist tool [3, 4].

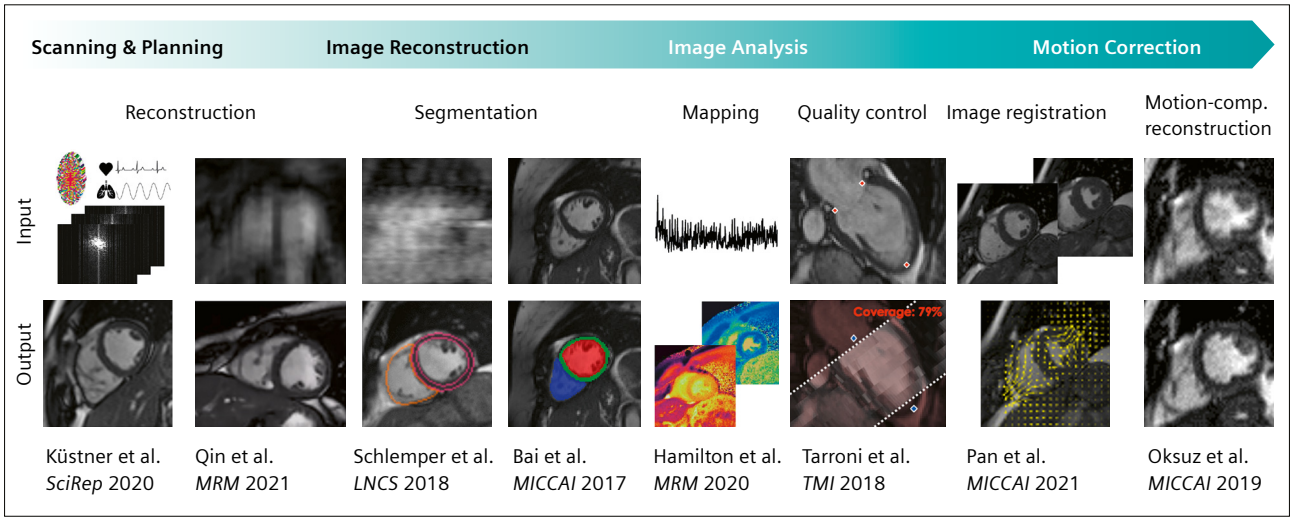

1 Overview of clinical workflow supported by several artificial intelligence (AI) methods. Different AI solutions along the imaging and processing chain are illustrated for cardiac cine imaging. The inputs and outputs of the proposed AI techniques are also shown.

Image reconstruction

Traditional image reconstruction techniques suffer from long reconstruction times and limitations in acceleration under Cartesian sampling patterns. Furthermore, prior knowledge of the reconstructed images needs to be incorporated into the reconstruction procedure. However, this prior information is often too simple to characterize the complex medical images. AI provides the opportunity to gain this prior knowledge directly from the data. Dictionary learning is an early example of data-driven learning in Compressed Sensing (CS)-based MRI reconstruction, and involves learning directly from undersampled data how the individual dictionary entries should be combined. AI-based solutions now achieve image quality similar or superior to classic CS-based approaches, while reducing the reconstruction time tremendously from minutes and hours to seconds. Furthermore, the learned priors can deal with the characteristic, coherent backfolding artifacts that appear in Cartesian sampling schemes, which are standard in the clinical workflow.

However, learning only a data-driven image prior is not enough, and special care needs to be taken with the acquired *k*-space data. While purely image-driven networks are able to produce realistic-looking images, the images themselves are not consistent with the acquired *k*-space data. We refer the interested reader to a previous article in MAGNETOM Flash and to book chapters [5, 6] for more information on how to include the acquired *k*-space into a reconstruction network. In the current article, we focus on the application of AI-based solutions to (high-dimensional) CMR, including static and dynamic imaging.

Fuin et al. proposed a multi-scale variational network for CMRA [7]. For this static application, the reconstruction time could be reduced from ~5 minutes for a CS-based approach to ~14 seconds for the proposed learning-based approaches. Comparable image quality was achieved between the fully sampled reference scan and the 9× accelerated scan. The results show that the acquisition time can be reduced from 18:55 minutes for the fully sampled reference scan to 2:34 minutes for the 9× accelerated acquisition, while the image quality stays comparable.

An alternative approach for shortening the scan time while simultaneously increasing spatial resolution is to use AI-based super resolution. Images are acquired at a low image resolution and retrospectively reconstructed to the high-resolution target. This approach has been successfully applied to cardiac cine [8, 9] and CMRA [10, 11].

In the context of cine image reconstruction, Schlemper et al. proposed a data-consistent convolutional neural network (CNN), performing alternating single-coil data-consistency steps and image denoising with a 5-layer CNN [12]. This approach was improved by a recurrent approach to propagate information through the time dimensions and between iterations [13]. Separated convolutions in the spatial domain and temporal domain further improve reconstruction quality, yielding more accurate functional

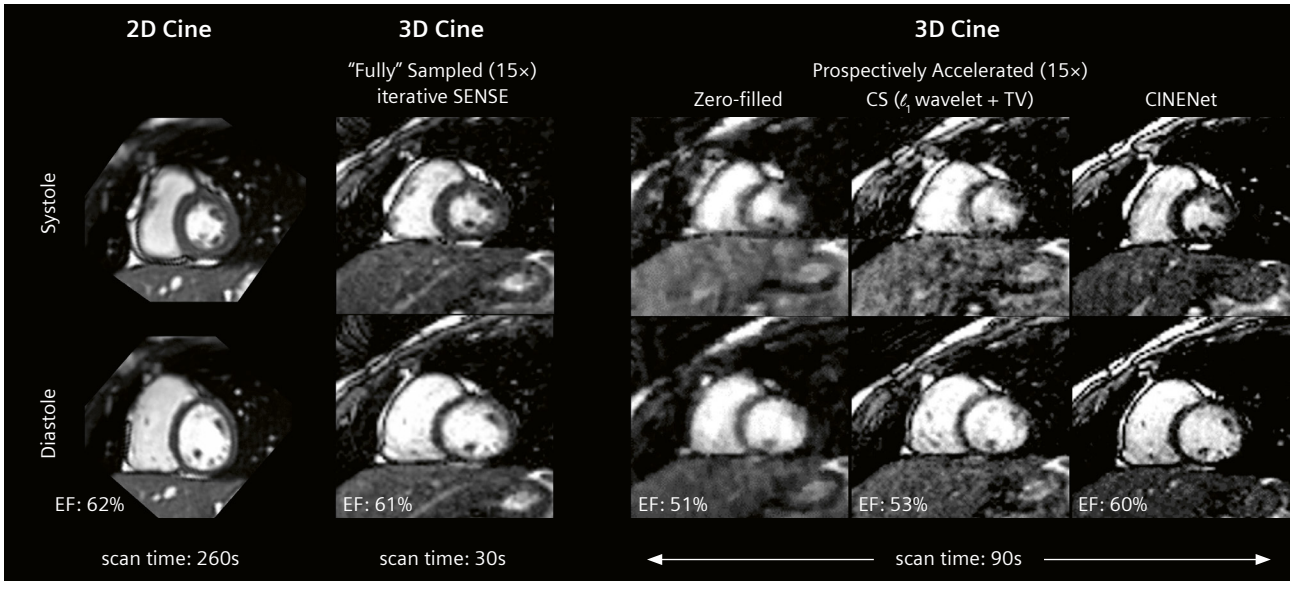

2 Physics-guided deep learning-based image reconstruction for cardiac cine imaging. High imaging acceleration (15×) enables the acquisition of a 3D cardiac cine with isotropic resolution and left ventricular coverage in a single breath-hold of < 10 seconds. A deep learning-based image reconstruction, CINENet, provides high image quality in contrast to the zero-filled reconstruction (input to network) or a Compressed Sensing (CS) reconstruction. CINENet reconstruction of accelerated scan (9 seconds) is in good accordance with a separate (slightly accelerated, 2.5×) 3D cine (30 seconds) and a conventional multi breath-hold 2D cine (260 seconds). The 3D cine with CINENet reconstruction shows high agreement with the conventional 2D cine in terms of left ventricular ejection fraction (EF).

parameters [14] and allowing for accelerated 3D cine reconstruction [15]. An example for accelerated single-breath-hold 3D cine reconstruction compared to conventional multi-slice multi-breath-hold 2D reconstruction is depicted in Figure 2. The aforementioned approaches operate directly on the full image, but low-rank and sparse priors are less frequently studied. Building on the success of unrolled networks, recent works focus on learning a structured low-rank prior [16] or low-rank plus sparse decomposition [17] in the context of dynamic MRI reconstruction.

While most approaches apply CNNs primarily in the image domain, hybrid networks exploit information in complementary domains. Due to the dynamic component in cine images, we can exploit the data in various domains. Exploiting all available data in various spaces pushes the reconstruction results further. El-Rewaidy et al. use both *k*-space and image domain information for radial imaging, implementing CNNs in both domains [18]. Complementary information in *k-t* and *x-f* space was studied in Qin et al. [19].

All aforementioned reconstruction approaches assume that fully sampled training data are available. The fully sampled data serve as a reference during training. However, training data is not always available, and is sometimes even impossible to acquire. Yaman et al. proposed a self-supervised learning approach that uses only the acquired training data points, with application to late gadolinium enhancement as depicted in Figure 3 [20]. The sampled data points are split into two disjoint sets, where the first set is used in the data consistency units of the unrolled reconstruction network, and the second set is used to evaluate the loss function during training directly in *k*-space.

Image analysis

CMR image segmentation and quantitative evaluation can be a challenging, time-consuming, and operator-intensive task. Segmentation of the chambers and myocardium is a mandatory postprocessing task. Automation of these tasks can therefore significantly reduce the time required for CMR image assessment.

AI-based solutions for image segmentation have been shown to be highly accurate and fast [21]. Considerable efforts have been directed toward cine imaging, as it is considered the gold standard for the assessment of cardiac chamber volumes and function [22]. The work of Morales et al. provided additional myocardial strain measures [23]. Segmentation methods have also been paired with predictions of important markers for cardiovascular disease, such as volume of pericardial adipose tissue [24] and scar-tissue areas [25]. Fahmy et al. automatically quantified left ventricular mass and scar volume in late gadolinium enhanced imaging [26], which showed strong agreement between the automated segmentations and the manual delineations. Farrag et al. [27] investigated the propagation of segmentation masks derived from cine imaging for the accurate segmentation of myocardial tissue in T1 mapping of a shMOLLI sequence. In contrast, the work of Hann et al. [28] segmented the myocardium directly in the shMOLLI data.

Segmentations have also been shown to provide valuable information for image reconstruction and motion correction tasks. Joint learning of motion estimation and segmentation for cine imaging was proposed by Qin et al. [29]. The results suggested that an efficient motion estimation network can bypass the need for high-quality reconstructions to achieve accurate image segmentation,

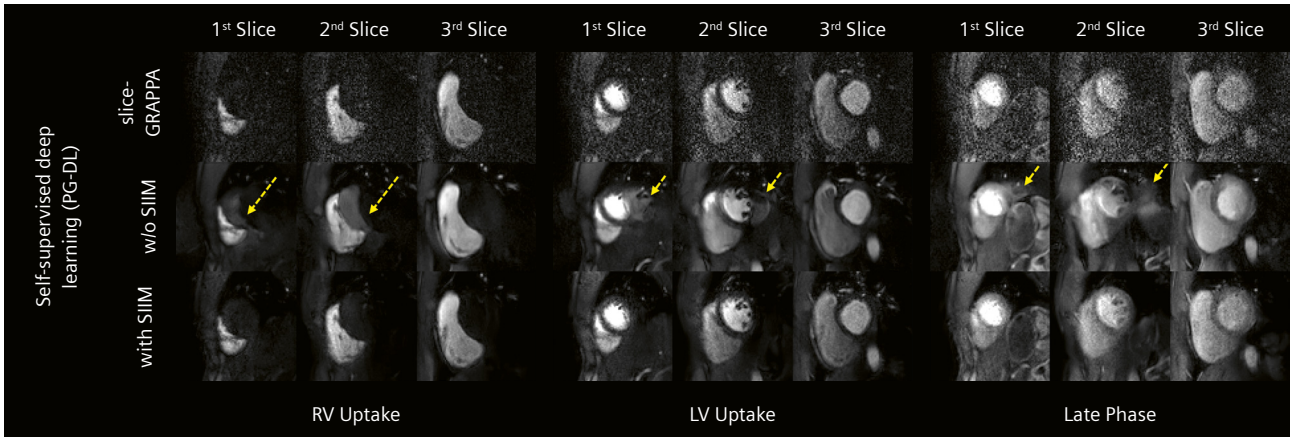

3 Physics-guided deep learning-based image reconstruction for dynamic contrast-enhanced MRI. A three-slice myocardial perfusion in the right ventricle (RV) uptake, left ventricle (LV) uptake and late phase is shown for different reconstruction techniques. A split slice-GRAPPA (top row) is compared to two self-supervised deep learning solutions (middle and bottom row) [63]. The difference between the deep learning methods is the use of signal intensity informed multi-coil (SIIM) encoding, which better models the underlying MR physics as indicated by the yellow arrows. *Image courtesy of Mehmet Akçakaya.*

indicating the superiority of high-dimensional data processing. Sun et al. [30] proposed a unified deep network architecture for joint image reconstruction and segmentation. The reconstruction and segmentation networks share network parts, acting as intrinsic regularizers for each other, while unshared network parts act specifically to the task (reconstruction or segmentation). Their results suggest that training a joint network is beneficial for high-quality segmentation of undersampled *k*-space data. While most multi-task networks aimed for an intermediate reconstructed image, Schlemper et al. [31] bypassed this step and directly predicted segmentation maps from highly undersampled dynamic CMR images of the UK Biobank data. Their results indicate that clinical parameters can be computed within an error of 10% if at least 10 lines are acquired for each cardiac phase using Cartesian sampling.

As sufficient image quality is a crucial factor in any further downstream task, Tarroni et al. devised an automated cardiac quality control [32]. The heart coverage, existence of inter-slice motion, and myocardial to blood pool contrast are automatically assessed. Their findings enable a reproducible and objective setting for large-scale and automated data processing.

Neural networks have also been proposed for quantitative CMR imaging to allow for accelerated myocardial tissue characterization. Jeelani et al. estimated quantitative T1 maps from a MOLLI sequence [33, 34]. The work of Fahmi et al. paired the quantification network with a segmentation to target the maps toward the myocardium [35].

For multi-parametric acquisitions in MR fingerprinting, AI solutions have been initially proposed for non-cardiac applications [36] in order to bypass dictionary simulation and pattern matching and thereby reduce computation time and memory requirements. In CMR fingerprinting, sequence timings depend on the subject's cardiac rhythm. Hamilton et al. proposed an estimation of T1 and T2 maps directly from undersampled spiral images showcasing rapid and robust predictions [37], as depicted in Figure 4.

Myocardial tissue characterization has also been studied in the context of radiomics. In radiomics, the image data is converted into mineable high-dimensional data using a large number of handcrafted features targeted toward the image intensity, and structural and textural information. These features are then used to perform segmentation of myocardial tissue [38], differentiate between acute and chronic infarction [39], differentiate between causes of myocardial hypertrophy [40], discriminate between hypertensive heart disease and hypertrophic cardiomyopathy patients [41], and quantify myocardial inflammation [42].

Beyond purely imaging-focused approaches, AI methods have also been used to predict outcomes in patients with various cardiovascular diseases [43] and identify relationships between cardiac morphology and non-imaging information as provided by genetic variations [44].

Motion correction

Physiological motion is still one of the major extrinsic sources of image artifacts and requires appropriate handling during acquisition or reconstruction. In the case of CMR, we are primarily dealing with respiratory and cardiac motion, which result in non-rigid deformations of the heart and its surrounding environment. Respiratory motion and cardiac motion are in most solutions regarded as periodic, but they do not necessarily have a fixed frequency throughout the scan. In other words, a subject might hold their breath, or a heartbeat might be skipped and should therefore be treated as cyclic rather than periodic. Simplifications in modeling and correcting motion may be necessary to handle the motion problem and to build an appropriate AI solution.

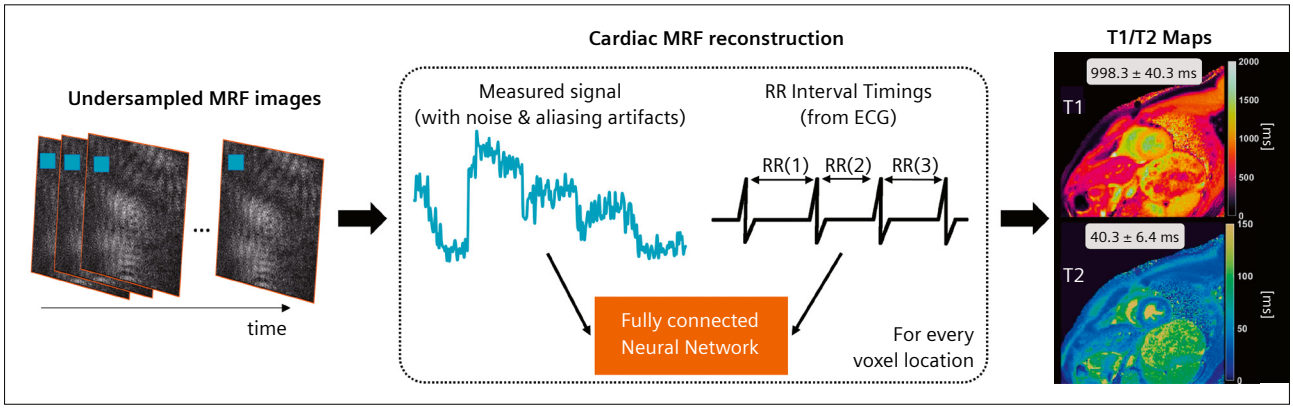

4 Deep learning-based magnetic resonance fingerprinting (MRF) for myocardial tissue mapping [37]. A cardiac MRF sequence collects data within an ECG-triggered window under breath-hold from which the temporal fingerprint (measured signal) can be extracted for every voxel location. Together with the heart-rate interval timings, a fully connected neural network estimates the T1 and T2 values at each voxel location. *Image courtesy of Jesse Hamilton.*

AI-based image registration methods have been proposed to map motion states in motion-resolved images, outputting a motion field of the moving anatomies. Mappings can be expressed between a pair of images (e.g., end-systolic frame to end-diastolic frame), known as pairwise registration, or between a group of images (several diastolic frames) to a target image (end-systolic frame), known as groupwise registrations. Large non-rigid motion across multiple temporal frames can occur, and in the case of 2D imaging the existence of through-plane motion complicates the motion estimation process. Moreover, estimated motion fields should be diffeomorphic, i.e., a forward motion (end-systolic to end-diastolic) can be easily inverted to a backward motion (end-diastolic to end-systolic).

A fast and reliable motion estimation is therefore required that correlates these short- and long-term correspondences. AI methods have been proposed to operate on the reconstructed motion-resolved images (i.e., in the image domain) for pairwise registrations [45–47] or groupwise registrations [48]. Alternatively, registration could be carried out directly on the acquired raw *k*-space data [49]. Since it is often of interest to estimate motion from as little data as possible (providing high temporal motion resolution), motion estimation procedures have been challenged with data from accelerated acquisitions [49–51].

Instead of outputting a motion field, joint motion-compensated image reconstruction networks have been studied. Motion estimations are embedded with the reconstruction process in order to exploit the high-dimensional data [52–54], as highlighted in Figure 5. Further combinations with segmentation have been studied in [55], which introduced a joint framework for motion artifact detection, correction in *k*-space, and image segmentation. In this setting, the motion correction problem is reformulated as a reconstruction task. The motion artifact network detects motion-affected lines in *k*-space, which are then signaled to the reconstruction part for removal, yielding a motion-corrected image from which segmentations are derived. The results showed that joint processing was superior to sequential processing.

Adversarial training strategies as proposed in [56, 57] aim to correct for the motion in the image domain. These networks consist of two parts: a generator network which predicts motion-corrected images from simulated motion-corrupted ones, and a discriminator which tries to distinguish between the generated motion-corrected images (from generator) and real motion-corrected images. The goal is to fool the discriminator network to generate images that look like real motion-corrected images. Alternatively, motion embeddings can be learned with variational autoencoders that allow to distinguish between motion-affected and motion-corrected scans [58].

Current challenges, opportunities, and limitations

CMR imaging offers a great opportunity for deep learning due to the redundancy and the high dimensionality of the data. However, we also face challenges regarding acquisition time, SNR, the trade-off between spatial and temporal resolutions, and different types of motion, e.g., cardiac and respiratory motion, which makes the application of deep learning techniques more demanding. While deep learning approaches often outperform CS-based approaches in terms of pixel-wise quantitative scores, these approaches might tend to over-blur the temporal component. However, a

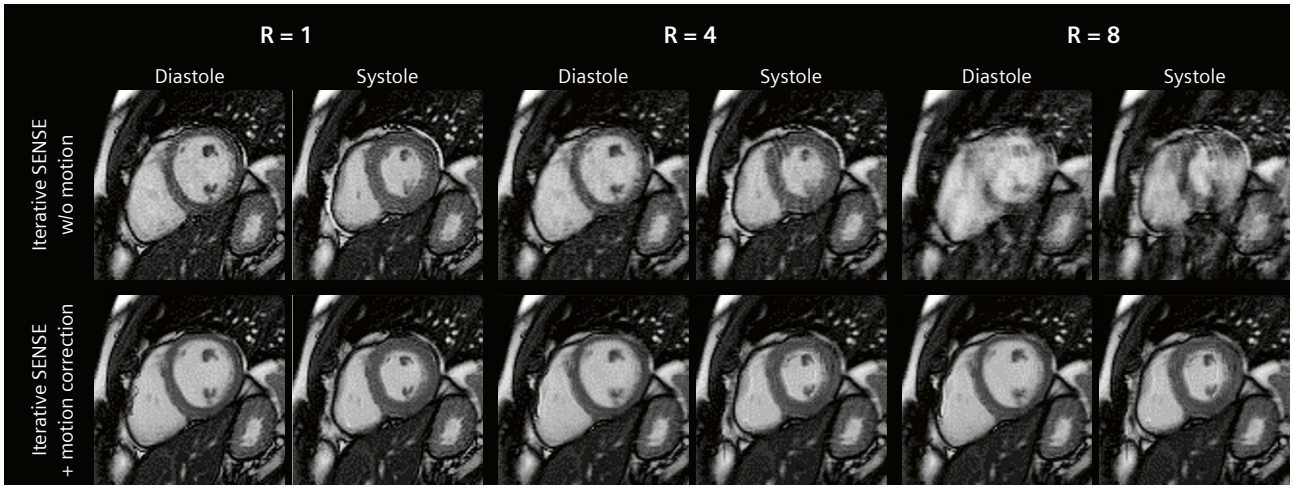

5 Motion-compensated image reconstruction for cardiac cine imaging. An image reconstruction is paired with a motion estimation network. The impact of sharing the available spatiotemporal information in a motion-corrected image reconstruction (bottom row) is shown in comparison to performing only a non-motion-informed image reconstruction (top row). For higher accelerations, sharing spatiotemporal data allows to increase sampling density and thereby improve image quality.

high resolution of the temporal dynamics is crucial for diagnosis and to detect subtle pathologies.

When using deep learning techniques, it is challenging to evaluate the quality and robustness of reconstruction approaches, especially in the case of subtle pathologies. However, we might get trapped in overly optimistic results if we use simulated data and neglect the unprocessed raw *k*-space data [59]. In a different line of work, the robustness of neural networks to small adversarial perturbations at the input was investigated [60]. Robustness of neural networks to changes in anatomy was studied in the context of static 2D imaging in [61], showing that domain shift has a marginal impact on image reconstruction when using unrolled networks and moderate acceleration. This observation regarding domain shift is different to image analysis tasks, where a subtle change might lead to mis-segmentation, for instance.

Deep learning approaches were intensively and individually studied in the context of scan planning, accelerated acquisition and reconstruction, and image analysis. While we often focus only on one part of this full imaging pipeline, deep learning provides many more opportunities to improve the whole workflow of CMR image acquisition for analysis and diagnosis. Future investigations of deep learning approaches will go deeper in supporting the choice of exam based on actual physiological scan parameters such as heart rate, or on the patient information obtained during the scan. Deep learning techniques will also support further acceleration in scan time to enable real-time interventional cardiac MRI [62]. We also observe a trend towards embedding different elements of the imaging pipeline into a deep learning approach and training this network end-to-end as shown in multi-task networks, or exploiting the available data, e.g., via motion fields, which will form the future of learning-based CMR imaging.

Acknowledgments

The authors would like to thank Jesse Hamilton and Mehmet Akçakaya for providing materials for the figures, and Teresa Correia, Tevfik Ismail, Wendy Strugnell, Chiara Coletti, Masa Bozic-Iven, Sebastian Weingärtner, and Gastao Cruz for the discussions.

References

1 Ismail TF, Strugnell W, Coletti C, Božić-Iven M, Weingärtner S, Hammernik K, et al. Cardiac MR: From Theory to Practice. Front Cardiovasc Med. 2022;9:826283.
2 Hammernik K, Kuestner T, Rueckert D. Machine Learning in MRI Reconstruction. In: Akcakaya M, Doneva M, Prieto C, editors. Magnetic Resonance Image Reconstruction Theory, Methods, and Applications. Elsevier; 2022. ISBN: 9780128227268. In press.
3 Thomas SJ, Bryant MG, Radvan J, Speier P, Mueller E, Schmidt M, et al. The need for speed – adenosine stress MRI in less than 30 minutes. J Cardiovasc Magn Reson. 2013;15(Suppl 1):E24.
4 Wang K, Zhang W, Li S, Bi X, Schmidt M, An J, et al. Free-Breathing 10-Min Cardiac MRI Protocol at 3.0t: Single-Center Experience. Biomedical Journal of Scientific & Technical Research. 2022;41(1):32365-32373.
5 Hammernik K, Knoll F, Rueckert D. Deep Learning for Parallel MRI Reconstruction: Overview, Challenges, and Opportunities. MAGNETOM Flash. 2019;75:10-15.
6 Hammernik K, Knoll F. Chapter 2 – Machine learning for image reconstruction. In: Zhou SK, Rueckert D, Fichtinger G, editors. Handbook of Medical Image Computing and Computer Assisted Intervention. Academic Press; 2020. p. 25–64.
7 Fuin N, Bustin A, Küstner T, Oksuz I, Clough J, King AP, et al. A multi-scale variational neural network for accelerating motion-compensated whole-heart 3D coronary MR angiography. Magn Reson Imaging. 2020;70:155–167.
8 Lin JY, Chang YC, Hsu WH. Efficient and Phase-aware Video Super-resolution for Cardiac MRI. arXiv. 10626 [eess.IV].
9 Steeden JA, Quail M, Gotschy A, et al. Rapid whole-heart CMR with single volume super-resolution. J Cardiovasc Magn Reson. 2020;22:56.
10 Küstner T, Munoz C, Psenicny A, Bustin A, Fuin N, Qi H, et al. Deep-learning based super-resolution for 3D isotropic coronary MR angiography in less than a minute. Magn Reson Med. 2021;86(5): 2837–2852.
11 Ishida M, Nakayama R, Uno M, et al. Learning-based super-resolution technique significantly improves detection of coronary artery stenoses on 1.5T whole-heart coronary MRA. J Cardiovasc Magn Reson. 2014;16 (Suppl 1), P218.
12 Schlemper J, Caballero J, Hajnal JV, Price AN, Rueckert D. A Deep Cascade of Convolutional Neural Networks for Dynamic MR Image Reconstruction. IEEE Trans Med Imaging. 2018;37(2):491–503.
13 Qin C, Schlemper J, Caballero J, Price AN, Hajnal JV, Rueckert D. Convolutional Recurrent Neural Networks for Dynamic MR Image Reconstruction. IEEE Trans Med Imaging. 2019;38(1):280–290.
14 Sandino CM, Lai P, Vasanawala SS, Cheng JY. Accelerating cardiac cine MRI using a deep learning-based ESPIRiT reconstruction. Magn Reson Med. 2021;85(1):152–167.
15 Küstner T, Fuin N, Hammernik K, Bustin A, Qi H, Hajhosseiny R, et al. CINENet: deep learning-based 3D cardiac CINE MRI reconstruction with multi-coil complex-valued 4D spatio-temporal convolutions. Sci Rep. 2020;10:13710.
16 Ke Z, Huang W, Cui ZX, Cheng J, Jia S, Wang H, et al. Learned Low-Rank Priors in Dynamic MR Imaging. IEEE Trans Med Imaging. 2021;40(12):3698–3710.
17 Huang W, Ke Z, Cui ZX, Cheng J, Qiu Z, Jia S, et al. Deep low-Rank plus sparse network for dynamic MR imaging. Medical Image Analysis. 2021;73:102190.
18 El-Rewaidy H, Fahmy AS, Pashakhanloo F, Cai X, Kucukseymen S, Csecs I, et al. Multi-domain convolutional neural network (MD-CNN) for radial reconstruction of dynamic cardiac MRI. Magn Reson Med. 2021;85(1):1195–1208.
19 Qin C, Duan J, Hammernik K, Schlemper J, Küstner T, Botnar R, et al. Complementary time-frequency domain networks for dynamic parallel MR image reconstruction. Magn Reson Med. 2021;86(6):3274–3291.
20 Yaman B, Shenoy C, Deng Z, Moeller S, El-Rewaidy H, Nezafat R, et al. Self-Supervised Physics-Guided Deep Learning Reconstruction for High-Resolution 3D LGE CMR. IEEE 18th International Symposium on Biomedical Imaging (ISBI), 2021, pp. 100–104.
21 Bernard O, Lalande A, Zotti C, Cervenansky F, Yang X, Heng PA, et al. Deep Learning Techniques for Automatic MRI Cardiac Multi-Structures Segmentation and Diagnosis: Is the Problem Solved? IEEE Trans Med Imaging. 2018;37(11):2514–2525.
22 Bai W, Sinclair M, Tarroni G, Oktay O, Rajchl M, Vaillant G, et al. Automated cardiovascular magnetic resonance image analysis

with fully convolutional networks.
J Cardiovasc Magn Reson. 2018;20(1):65.
23 Morales MA, van den Boomen M, Nguyen C, Kalpathy-Cramer J, Rosen BR, Stultz CM, et al. DeepStrain: A Deep Learning Workflow for the Automated Characterization of Cardiac Mechanics. Front Cardiovasc Med. 2021;8:730316.
24 Bard A, Raisi-Estabragh Z, Ardissino M, Lee AM, Pugliese F, Dey D, et al. Automated Quality-Controlled Cardiovascular Magnetic Resonance Pericardial Fat Quantification Using a Convolutional Neural Network in the UK Biobank. Front Cardiovasc Med. 2021;8:677574.
25 Chen J, Yang G, Gao Z, Ni H, Angelini E, Mohiaddin R, et al. Multiview two-task recursive attention model for left atrium and atrial scars segmentation. arXiv:1806.04597 [cs.CV].
26 Fahmy AS, Rausch J, Neisius U, Chan RH, Maron MS, Appelbaum E, et al. Automated Cardiac MR Scar Quantification in Hypertrophic Cardiomyopathy Using Deep Convolutional Neural Networks. JACC Cardiovasc Imaging. 2018;11(12):1917–1918.
27 Farrag NA, White JA, Ukwatta E. Semi-automated myocardial segmentation in native T1-mapping CMR using deformable non-rigid registration of CINE images. In: Medical Imaging 2019: Biomedical Applications in Molecular, Structural, and Functional Imaging. SPIE Conference Series. 2019;10953.
28 Hann E, Ferreira VM, Neubauer S, Piechnik SK. Deep Learning for Fully Automatic Contouring of the Left Ventricle in Cardiac T1 Mapping. CMR 2018 – A Joint EuroCMR/SCMR Meeting Abstract Supplement. ID# 376365.
29 Qin C, Bai W, Schlemper J, Petersen SE, Piechnik SK, Neubauer S, et al. Joint Learning of Motion Estimation and Segmentation for Cardiac MR Image Sequences. arXiv;2018.1806.04066 [cs.CV].
30 Sun L, Fan Z, Ding X, Huang Y, Paisley J. Joint CS-MRI Reconstruction and Segmentation with a Unified Deep Network. Lecture Notes in Computer Science (including subseries Lecture Notes in Artificial Intelligence and Lecture Notes in Bioinformatics). 2019;11492 LNCS:492-504.
31 Schlemper J, Oktay O, Bai W, Castro DC, Duan J, Qin C, et al. Cardiac MR Segmentation from Undersampled *k*-space Using Deep Latent Representation Learning. In: Frangi A, Schnabel J, Davatzikos C, Alberola-López C, Fichtinger G (eds). Medical Image Computing and Computer Assisted Intervention – MICCAI 2018. MICCAI 2018. Lecture Notes in Computer Science. 2018;11070.
32 Tarroni G, Bai W, Oktay O, Schuh A, Suzuki H, Glocker B, et al. Large-scale Quality Control of Cardiac Imaging in Population Studies: Application to UK Biobank. Sci Rep. 2020;10:2408.
33 Jeelani H, Yang Y, Zhou R, Kramer CM, Salerno M, Weller DS. A Myocardial T1-Mapping Framework with Recurrent and U-Net Convolutional Neural Networks. In: IEEE 17th International Symposium on Biomedical Imaging (ISBI). 2020:1941–1944.
34 Martini N, Della Latta D, Santini G, Valvano G, Barison A, Avogliero F, et al. Automatic AHA model segmentation of cardiac T1 maps with deep learning. Proc Intl Soc Mag Reson Med. 2018;26:1047.
35 Fahmy AS, El-Rewaidy H, Nezafat M, Nakamori S, Nezafat R. Automated analysis of cardiovascular magnetic resonance myocardial native T1 mapping images using fully convolutional neural networks. J Cardiovasc Magn Reson. 2019;21(1):7.
36 Cohen O, Zhu B, Rosen MS. MR fingerprinting Deep RecOnstruction NEtwork (DRONE). Magn Reson Med. 2018;80(3):885–894.
37 Hamilton JI, Currey D, Rajagopalan S, Seiberlich N. Deep learning reconstruction for cardiac magnetic resonance fingerprinting T1 and T2 mapping. Magn Reson Med. 2021;85(4):2127–2135.
38 Kotu LP, Engan K, Skretting K, Måløy F, Orn S, Woie L, et al. Probability mapping of scarred myocardium using texture and intensity features in CMR images. Biomed Eng Online. 2013;12:91.
39 Larroza A, López-Lereu MP, Monmeneu JV, Gavara J, Chorro FJ, Bodí V, et al. Texture analysis of cardiac cine magnetic resonance imaging to detect nonviable segments in patients with chronic myocardial infarction. Med Phys. 2018;45(4):1471–1480.
40 Schofield R, Ganeshan B, Kozor R, Nasis A, Endozo R, Groves A, et al. CMR myocardial texture analysis tracks different etiologies of left ventricular hypertrophy. J Cardiovasc Magn Reson. 2016;18(Suppl 1):O82.
41 Neisius U, El-Rewaidy H, Nakamori S, Rodriguez J, Manning WJ, Nezafat R. Radiomic Analysis of Myocardial Native T1 Imaging Discriminates Between Hypertensive Heart Disease and Hypertrophic Cardiomyopathy. JACC Cardiovasc Imaging. 2019;12(10):1946–1954.
42 Baeßler B, Schaarschmidt F, Treutlein M, Stehning C, Schnackenburg B, Michels G, et al. Re-evaluation of a novel approach for quantitative myocardial oedema detection by analysing tissue inhomogeneity in acute myocarditis using T2-mapping. Eur Radiol. 2017;27(12):5169–5178.
43 Kotu LP, Engan K, Borhani R, Katsaggelos AK, Ørn S, Woie L, et al. Cardiac magnetic resonance image-based classification of the risk of arrhythmias in post-myocardial infarction patients. Artif Intell Med. 2015;64(3):205–15.
44 Biffi C, de Marvao A, Attard MI, Dawes TJW, Whiffin N, Bai W, et al. Three-dimensional cardiovascular imaging-genetics: a mass univariate framework. Bioinformatics. 2018;34(1):97–103.
45 Pan J, Rueckert D, Kuestner T, Hammernik K. Efficient Image Registration Network for Non-Rigid Cardiac Motion Estimation. In: Haq N, Johnson P, Maier A, Würfl T, Yoo J (eds). Machine Learning for Medical Image Reconstruction. MLMIR 2021. Lecture Notes in Computer Science. 2021;12964. Springer, Cham.
46 Morales MA, Izquierdo-Garcia D, Aganj I, Kalpathy-Cramer J, Rosen BR, Catana C. Implementation and Validation of a Three-dimensional Cardiac Motion Estimation Network. Radiol Artif Intell. 2019;1(4):e180080.
47 Upendra RR, Wentz BJ, Shontz SM, Linte CA. A Convolutional Neural Network-based Deformable Image Registration Method for Cardiac Motion Estimation from Cine Cardiac MR Images. Comput Cardiol (2010). 2020;47:10.22489/CinC.2020.204.
48 Qi H, Hajhosseiny R, Cruz G, Küstner T, Kunze K, Neji R, et al. End-to-end deep learning nonrigid motion-corrected reconstruction for highly accelerated free-breathing coronary MRA. Magn Reson Med. 2021;86(4):1983–1996.
49 Küstner T, Pan J, Qu H, Cruz G, Gilliam C, Blu T, et al. LAPNet: Non-Rigid Registration Derived in *k*-Space for Magnetic Resonance Imaging. In: IEEE Transactions on Medical Imaging. 2021;40(12):3686–3697.
50 Hammernik K, Pan J, Rueckert D, Küstner T. Motion-Guided Physics-Based Learning for Cardiac MRI Reconstruction. In: 55th Asilomar Conference on Signals, Systems, and Computers. 2021:900–907.
51 Huttinga NRF, van den Berg CAT, Luijten PR, Sbrizzi A. MR-MOTUS: model-based non-rigid motion estimation for MR-guided radiotherapy using a reference image and minimal *k*-space data. Phys Med Biol. 2020;65(1):015004.
52 Seegoolam G, Schlemper J, Qin C, Price A, Hajnal J, Rueckert D. Exploiting Motion for Deep Learning Reconstruction of Extremely-Undersampled Dynamic MRI. In: Shen D, Liu T, Peters TM, Staib LH, Essert C, Zhou S, et al. (eds). Medical Image Computing and Computer Assisted Intervention – MICCAI 2019. MICCAI 2019. Lecture Notes in Computer Science. 2019;11767. Springer, Cham.
53 Küstner T, Pan J, Gilliam C, Qi H, Cruz G, Hammernik K, et al. Self-Supervised Motion-Corrected Image Reconstruction Network for 4D Magnetic Resonance Imaging of the Body Trunk. APSIPA Transactions on Signal and Information Processing. 2022;11(1):e12.

54 Qi H, Hajhosseiny R, Cruz G, Kuestner T, Kunze K, Neji R, et al. End-to-end deep learning nonrigid motion-corrected reconstruction for highly accelerated free-breathing coronary MRA. Magn Reson Med. 2021;86(4):1983–1996.
55 Oksuz I, Clough JR, Ruijsink B, Anton EP, Bustin A, Cruz G, et al. Deep Learning-Based Detection and Correction of Cardiac MR Motion Artefacts During Reconstruction for High-Quality Segmentation. IEEE Trans Med Imaging. 2020;39(12):4001–4010.
56 Zhang Y, Zhang W, Zhang Q, Yang J, Chen X, Zhao S. CMR motion artifact correction using generative adversarial nets. arXiv:1902.11121 [cs.CV].
57 Küstner T, Armanious K, Yang J, Yang B, Schick F, Gatidis S. Retrospective correction of motion-affected MR images using deep learning frameworks. Mag Reson Med. 2019;82(4):1527-1540.
58 Ghodrati V, Bydder M, Ali F, Gao C, Prosper A, Nguyen KL, et al. Retrospective respiratory motion correction in cardiac cine MRI reconstruction using adversarial autoencoder and unsupervised learning. NMR Biomed. 2021;34(2):e4433.
59 Shimron E, Tamir JI, Wang K, Lustig M. Implicit data crimes: Machine learning bias arising from misuse of public data. Proc Natl Acad Sci U S A. 2022;119(13):e2117203119.
60 Antun V, Renna F, Poon C, Adcock B, Hansen AC. On instabilities of deep learning in image reconstruction and the potential costs of AI. Proc Natl Acad Sci U S A. 2020;117(48):30088–30095.
61 Hammernik K, Schlemper J, Qin C, Duan J, Summers RM, Rueckert D. Systematic evaluation of iterative deep neural networks for fast parallel MRI reconstruction with sensitivity-weighted coil combination. Magn Reson Med. 2021;86(4):1859–1872.
62 Jaubert O, Montalt-Tordera J, Knight D, Coghlan GJ, Arridge S, Steeden JA, et al. Real-time deep artifact suppression using recurrent U-Nets for low-latency cardiac MRI. Magn Reson Med. 2021;86(4):1904–1916.
63 Yaman B, Hosseini SAH, Moeller S, Ellermann J, Uğurbil K, Akçakaya M. Self-supervised learning of physics-guided reconstruction neural networks without fully sampled reference data. Magn Reson Med. 2020;84(6):3172–3191.

Contact

Kerstin Hammernik, Ph.D.
AI in Healthcare and Medicine
Technical University of Munich
Boltzmannstr. 3
85748 Garching
Germany
k.hammernik@tum.de

Thomas Küstner, Ph.D.
University Hospital Tübingen
Hoppe-Seyler-Straße 3
72076 Tübingen
Germany
thomas.kuestner@med.uni-tuebingen.de

Meet Siemens Healthineers

Siemens Healthineers: Our brand name embodies the pioneering spirit and engineering expertise that is unique in the healthcare industry. The people working for Siemens Healthineers are totally committed to the company they work for, and are passionate about their technology. In this section we introduce you to colleagues from all over the world – people who put their hearts into what they do.

Yoshiaki Komori

Yoshiaki Komori grew up in Yokohama, a city near Tokyo in Japan. He received an M.Sc. from the Nuclear Engineering Research Institute at Tokyo Institute of Technology. He studied in the Thermal Fluid Dynamics Laboratory, focusing on cooling technology for nuclear reactor fuel rods.

After graduating, Yoshiaki worked at Tsukuba Space Center, part of the National Space Development Agency of Japan. He was involved in space-shuttle missions and the International Space Station (ISS) assembly mission for Japanese astronaut projects. His work on ISS missions at the Johnson Space Center taught him how enjoyable it can be to work for an international company.

In 2001, Yoshiaki joined Siemens Healthcare K.K. as an MR application specialist. It was here that he began his career in medical engineering. At the time, non-contrast MR angiography (MRA) techniques were being actively researched in Japan, and he supported the development of non-CE whole heart coronary MRA and sequences such as NATIVE SPACE and NATIVE TrueFISP. He also helped to communicate Japanese MR trends to the world. Yoshiaki has now worked for over 20 years as a scientist and collaboration manager in the cardiovascular research field. In 2023, he became head of the MR Research and Collaboration Department at Siemens Healthcare K.K., Japan.

How did you first come into contact with MRI?
I had actually never heard of an MRI scanner until I joined Siemens. I had knowledge of nuclear physics for nuclear reactors, but during my on-the-job training in the MR application team, I remember being very surprised about how clearly the human body could be visualized using nuclear magnetic resonance. In the world of fluid dynamics, laser Doppler velocimeters (LDV) and ultrasonic velocity profilers (UVP) were the main instruments used for flow visualization, so I was surprised to learn about the principles of blood flow imaging such as time-of-flight MRA and phase-contrast MRA. To me, an MRI machine looked like a giant measuring device for flow velocity.

What do you find motivating about your job?
The ability to share with the world the results that Japanese cardiovascular MRI researchers produce using the latest technology from Siemens Healthineers. Japanese radiologists have a strong preference for MR imaging of the highest quality, right down to the smallest detail. They also have a wealth of scanning knowledge and expertise. On the other hand, there aren't many positions for MRI physicists in Japanese hospitals.

To achieve good results, we need to combine a good research skills with good operating and engineering skills. The collaboration manager at Siemens Healthineers fits into this critical mix as an MRI expert. The customer is the medical expert. We work together to produce good research results. This type of teamwork is very rewarding.

Sometimes I encounter things I don't understand and it becomes hard to make a decision. At such times, our overseas colleagues help me. In fact, many engineers have helped me over the past 20 years. Their support has been invaluable whenever I've faced a challenging situation.

What are the biggest challenges in your job?
MRI research has a long history, but for most of that time, the neuro and body research fields have been the mainstream. The history of research in the cardiovascular field is not so long. When I started cardiovascular MRI research in 1999, the late gadolinium enhancement (LGE) imaging method was just emerging, and the clinical usefulness of cardiovascular MRI was just beginning to be investigated. Recently, studies such as free-breathing cardiac imaging methods have begun, but I believe there is still room for further developing cardiovascular MRI as a routine examination in clinical settings in Japan.

My challenges are to promote the clinical use of cardiovascular MRI more widely, and to advocate for cardiovascular MRI among young researchers, so they will enter this exciting field.

What would you do if you could spend a month doing whatever you wanted?
If I could take a month-long vacation, I would like to get a small boat license and go fishing with my son. As you all know, Japan is surrounded by the sea. Ocean currents are abundant here. It's perfect for fishing and then eating sashimi. And of course we can enjoy a hot spring afterward!

Get to know us

Michaela Schmidt
Erlangen, Germany

Peter Speier, Ph.D.
Erlangen, Germany

Carmel Hayes
Erlangen, Germany

Christian Geppert, Ph.D.
Erlangen, Germany

Solenn Toupin, Ph.D.
Bordeaux, France

Kelvin Chow, Ph.D.
Chicago, USA

Find more portraits of our colleagues around the world!

www.magnetomworld.siemens-healthineers.com/meet-siemens-healthineers

Not for distribution in the US

On account of certain regional limitations of sales rights and service availability, we cannot guarantee that all products included in this brochure are available through the Siemens Healthineers sales organization worldwide. Availability and packaging may vary by country and is subject to change without prior notice. Some/All of the features and products described herein may not be available in the United States.

The information in this document contains general technical descriptions of specifications and options as well as standard and optional features which do not always have to be present in individual cases, and which may not be commercially available in all countries. Due to regulatory reasons their future availability cannot be guaranteed. Please contact your local Siemens organization for further details.

Siemens Healthineers reserves the right to modify the design, packaging, specifications, and options described herein without prior notice. Please contact your local Siemens Healthineers sales representative for the most current information.

Note: Any technical data contained in this document may vary within defined tolerances. Original images always lose a certain amount of detail when reproduced.

Siemens Healthineers Headquarters
Siemens Healthcare GmbH
Henkestr. 127
91052 Erlangen, Germany
Phone: +49 9131 84-0
siemens-healthineers.com

Published by Siemens Healthcare GmbH · Order No. A91MR-1000-190C-7600 ·